Final Design Review

Team name: ReSAT Team

Country: Poland

"The people who are crazy enough
to think they can change the world
are the ones who do."

-Steve Jobs

Table of Contents

1 CHANGELOG

Critical Design Review

- Section 3.2 was updated by:
  - adding a mounting spot for a magnet on the rotary disk for RPM reading.
  - changing the CanSat's material from PA12-CF to PC for more reliable radio connectivity.
  - splitting the model into several parts for easier assembly.
  - removing material from the blades for carbon rod insertion.
  - introducing an additional buffer in the battery holder to minimise vibrations.
  - adding special rails for easy access to the PCB.
- Section 3.3 was updated by:
  - changing the step-down voltage converter TPS54331DR to a step-up/step down converter Pololu 4941.
  - changing USB-micro to USB-C for higher data transfer speed.
  - introducing the ADS1115IDGSR analog to digital converter for higher accuracy and less pins used.
  - adding the GL5516 photoresistor as a reliable way of detecting exit from the rocket.
  - adapting simplified electronics diagram to accommodate electronic component changes.
  - replacing the BMP280 and HDC1080DMBR with the more capable BME280 to reduce space-usage and increase quality.
  - changing the GPS from PA1616D to the PA1010D for its improved accuracy and better satellite acquisition capabilities as well as I^2C capabilities.
  - replacing MCP1640B-I/MC supercapacitor step-up converter with U1V11A capable of starting at lower voltage
  - choosing a 220F capacitor over a 250F one due to lower price and more compact package.
  - introducing external voltage converters to save space on the PCB and increase reliability.
  - adding a HX6659IUA-B Hall effect sensor to read relative rotational speed between the parachute and CanSat body.
  - introducing power source switching, from the battery to the secondary mission supercapacitor, as an additional feature to increase the potential runtime of the CanSat.
  - adding battery capacity sensing for improved reliability of the system.
  - adding capacitors next to crucial electrical components to provide enough current during power consumption spikes.
  - changing antenna model to ATK-10/400-470 MHz.
- Section 3.4 was updated by:
  - revising the program flow and data handling schemas to accommodate the changes made in Section 3.3.

    - reading altitude from the PA1010D, when available, instead of calculating it from the air pressure for increased accuracy while maintaining reliability.
    - introducing the option of measuring angular speed using the HX6659IUA-B Hall effect sensor and a magnet in the rotary disk for more useful data.
    - switching the development environment from Visual Studio Code and the ESP-IDF to the Arduino IDE and open-source libraries for easier cooperation within the software team.
- Section 3.5 was updated by:
    - including the parachute's area after simulations.
    - adding the parachute's 3D model for easier visualisation.
- Sections 5.1 and 5.2 were updated to reflect the team's project completion progress.
- Section 5.3 was updated to reflect the changes made in Sections 3.2 and 3.3 and sponsorships.
- Section 6 was updated to reflect the team's outreach programme progress.

Final Design Review

- Section 3.1 was updated by removing the no longer necessary servomechanism.
- Section 3.2 was updated by:
    - adding clearances between parts for easier printing.
    - redesigning the bottom cover by including the aperture for switches, USB and SD ports.
    - redesigning the top cover to strengthen the connection of the hull parts.
    - testing the model tolerances through realistically modelling the non-printable parts.
    - adding heat-set threaded inserts which strengthen screw connections.
    - removing the springs that open the propeller blades, since the test had shown that they are not required to open the blades while falling.
    - updating the parachute's mounting by changing the attachment of strings.
    - adding a slot for a nut and a hole for set screw for a secure connection between the motor shaft and adapter.
    - adding a GPS module mounting spot for more accurate positioning.
    - including a ball bearing in the propeller's opening mechanism to minimize the friction for optimal propeller unfolding.
    - simplifying the assembly by redesigning all parts.
    - printing the hinge out of PC instead of metal machining since tests have proven that it is unnecessary.
- Section 3.3 was updated by:
    - adding flexible PCBs.
    - replacing the BME280 with the BMP581 and TMP117 for more accurate readings.
    - removing the step up converter and directly powering the capacitor from the motor to lower losses and increase end energy.
    - updating the power consumption estimates to accommodate the changes made.
    - choosing the PHB-5R0V505-R supercapacitor over the HS1625-3R8227-R.
    - describing the reasoning behind choosing the new supercapacitor based on analysing a RC circuit.

- Section 3.4 was updated by:
  - updating block diagrams to represent the changes made in Sections 3.2 and 3.3.
  - summarizing all of the wired and wireless data transfers for readability.
  - describing the ground station software and live dashboard.
- Section 3.5 was updated by:
  - choosing a more vibrant color for the parachute for easier recovery.
  - further describing the mounting system used to connect the parachute to the adapter.
- Section 3.6 was updated by replacing individual components with the same PCB as the one used as an onboard computer.
- Section 4.1 was updated by removing the servomechanism test.
- Section 4.2 was updated by conducting and describing more accurate primary mission sensor tests to ensure full reliability.
- Section 4.3 was updated by redoing the dynamo tests with more data collected.
- Section 4.4 was updated by:
  - redoing the mass balance with the final version of the CanSat.
  - checking the strength of the newly inserted carbon rods.
  - updating the mass table - model geometry change, added bearings, different antenna, more screws, parachute (added snap swivels)
  - balancing out the previously uneven mass distribution
- Section 4.5 was updated by performing a more comprehensive communication system test.
- Section 4.6 was updated by:
  - including screenshots with the physics parameters of the CFD simulations.
  - redoing the CFD with more accurate parameters (enhanced meshing).
  - collecting and comparing rate of descent data from multiple drop tests.
- Section 4.7 was updated by conducting a full battery test.
- Section 4.8 was added to summarize all of the holistic high-altitude tests.
- Section 5.1 was updated to reflect the team's project completion progress.
- Section 5.3 was added to highlight the ReSat principles.
- Section 5.4 was updated to reflect the changes made in Sections 3.2 and 3.3 and sponsorships.
- Section 6 was updated to reflect the team's outreach programme progress.
- Section 7 was added to easily summarise the CanSat's physical characteristics.

2 Introduction

2.1 The Team

The team consists of five students from four schools across two countries. Part of them competed in this competition last year and the other half met at the Adamed SmartUp summer science camp, a highly selective Polish STEM scholarship programme. Given shared interests in the fields of science, technology, engineering, and mathematics, the decision to participate in ESERO CanSat was made. It was obvious that **collaborating across country borders** and different time zones would prove to be challenging, nevertheless, the team members decided that it was a great opportunity to familiarise themselves with **long-distance** transnational collaboration, emulating the day-to-day operations of an international organization or corporation like **ESA**. Since each member wholeheartedly believes that the best way to learn is through practice, they view this competition as the perfect opportunity to push themselves out of their comfort zones and broaden their horizons.

2.2 Organisation and Roles

The responsibilities have been divided evenly among all of the team members and a team leader has been chosen, keeping in mind personal interests, skills, and achievements within certain fields. The team's main center of communication is a Discord server but a Jira project has also been created to track progress and delegate tasks and a Google Drive has been made to facilitate easier virtual cooperation and file access. All of the work happens outside of school with everyone committing an average of 8 hours per week.

Because of the different sets of skills, and interests in the team, the team has been divided into four groups:

- **Software Team** (Miron with Michał Mrzyk's support) creating software for the mission.
- **Electronic & Mechanical Team** (Maciej and Jan) designing the electronic system and construction of the satellite.
- **Recovery Team** (Michał Mueller) constructing the rotafoil parachute.
- **Outreach Team** (Jan with Miron's support) popularizing the project and educating the masses.

Below, the team's tutor and each team member has written a short description:

Marcin Wygaś (tutor)

I am an IT teacher at **V High School and Mechanical-Technical School in Bielsko-Biała**. I take my role as an educator seriously and support my students both at school and outside of it. I am interested in cybersecurity, 3D printing, Arudino, and SDR. Throughout this project, my role will include supporting the team with my experience and knowledge. I plan to commit roughly three hours per week, with two of them being at school.

Michał Mueller (team leader)

Thanks to the Polish Scholarship Scheme, I am a lower sixth-form student at **Worth School, England**, pursuing the IB DP with higher-level subjects in Mathematics, Physics, and Economics. My academic interests are in STEM, and I enjoy learning languages and playing the piano in my free time. As the group leader for this project, I oversee the recovery system and team management while supporting the software designers. This competition grants a valuable opportunity to develop my engineering skills.

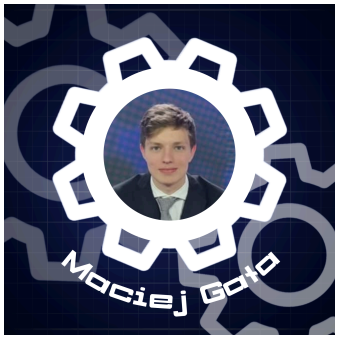

Maciej Gała

I am currently in my third year at **V High School in Bielsko-Biała**. My class profile is mathematics-physics-IT however I am mainly focused on physics. My interests are mechanical and electrical engineering which I take great pleasure applying in automating my growing 3D print farm. Apart from that I am keen on sports such as football, table tennis and volleyball. In the project, I am in charge of the electrical design and assistance with the CAD model.

Michał Mrzyk

Since the beginning of primary school, I have always been interested in astronomy and astronautics. Currently, I am in the third year of **V High School in Bielsko-Biała**, where I am developing my passion for physics and programming. Also I am keen on making films and sports for instance volleyball and cycling. With this project, I want to improve my skills in engineering. In the team, I am responsible for physical description, calculations, data analysis, and software support.

Miron Kobylański

I am currently a junior at **XXXIII Copernicus High School in Warsaw** and have recently started my first year of the IB DP, taking higher-level courses in Mathematics, Physics, and German. My interests lie in computer science, robotics, computer hardware, and machine learning but I also enjoy sports (cycling, rowing), as well as non-STEM extracurriculars (Model United Nations, language learning). Within this project I am mainly responsible for the software, for instance, collecting and processing the data from various sensors and displaying it visually.

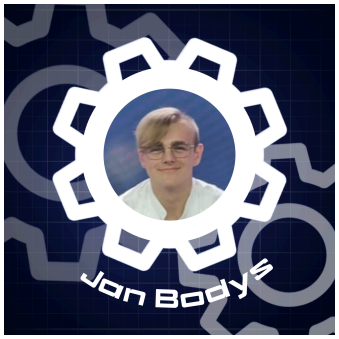

Jan Bodys

I am a third-grade **Mechatronics student at the Electronic Technical High School in Szczecin**, interested in robotics, device construction, and astronomy. As part of the ReSAT Team, I manage 3D modeling, mechanical innovations, and the CanSat case design, along with social media and graphics, including our logo and Instagram. I enjoy mountain hiking, wood carving, and aim to design tools to improve lives while developing my skills through competitions.

2.3 Mission Objectives

The **primary mission** will be studying air pressure and temperature in relation to the altitude of the satellite. After collecting the data, dynamic graphs will be plotted at the ground station. The mission has been split into 5 distinct phases visible in **Figure 1**.

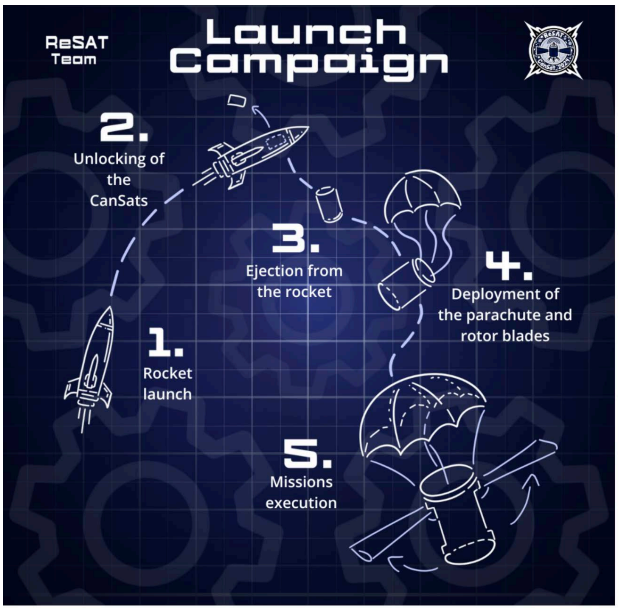

Figure 1 – Illustration of the mission phases

The **secondary mission's** objective is to prove that converting energy from the satellite's freefall is possible and to safely store it. After further refinement, the energy generated by this technology could potentially serve as the sole power source of an entire mission. In order to generate the necessary rotational velocity difference a rotor parachute will be used, effectively spinning counterclockwise, with the main body rotating clockwise thanks to retractable propeller blades. As the hypothesis, the influence of atmospheric pressure on the energy absorbed will be investigated.

Airflow during freefall is almost always perceived as a natural consequence or obstacle, however, it can be viewed not as a disadvantage but as a possibility. Not only does this approach allow energy, which would otherwise be wasted, to be conserved, adhering to the principles of the worldwide sustainability movement and the Sustainable Development Goals, but also allows the Can to utilise this stored energy to power itself even longer or allow high energy-consuming devices to function, when they otherwise could not, due to the limited capacity of onboard batteries. This mission will prove whether it is physically possible to transform enough energy to fulfill the power drain or solely to support the accumulators, which is especially important in the case of space or weight restrictions. The following three criteria must be met for the mission to be considered successful:

- **The propeller blades and parachute should deploy safely.**
- **The parachute and the body should spin in the previously decided opposite directions.**
- **Electricity should be generated and stored onboard the CanSat.**

This technological solution will be possible since similar systems are currently installed on commercial airplanes. When the vehicle is in danger of energy shortage due to engine malfunction a system called the Ram Air Turbine is deployed. It consists of a turbine connected to an electrical generator. Relative airflow causes spinning which is transferred into electrical current, which maintains crucial systems.

The results of this research project might be relevant in other missions as well as the exploration of planets with an atmosphere. On space probes, energy is the most crucial element, as it forces the most energy-consuming devices to function in intervals due to the limited size of accumulators. This mission will show how much energy freefall can generate and how to implement it in different atmospheric conditions.

3 CanSat Description

3.1 Mission Overview

The mission focuses on building a CanSat mini-satellite, which is to be launched onboard a rocket to an altitude of roughly 1-2km. Upon exiting the rocket, a **rotafoil parachute** will be unfolded by the air drag.

The parachute will be tied to the **stopper** of the propeller blades to prevent jamming inside the rocket and its initial drag will be used to remove it, effectively releasing the propeller blades. There will be four blades in total for additional stability and rotational speed. The parachute will transmit rotational velocity to the motor shaft through a rotary disk mechanism. The suspension lines will be constructed from **braided steel wire** and kept as short as functionally possible to minimize the risk of entanglement, ensure efficient energy transfer, and facilitate safe deployment of the parachute. Each line will be equipped with a snap connector at one end and a swivel at the other, allowing for secure attachment to the disk and enabling quick and easy disassembly.

Equipped with both digital and analog sensors, the CanSat will measure temperature, air pressure, light level, GPS coordinates, rotational data in all axes, acceleration, power output of the power generator and battery, as well as the relative angular speed between the parachute and the CanSat body. All sensor and GPS data will be sent live to the ground station via radio antenna. Additionally, during the flight, sensor data will be collected and stored on an SD card.

3.2 Mechanical/Structural Design

In order to complete the secondary mission, the main body of CanSat has four propeller blades (**NACA4412** airfoil shape), ensuring that the air drag force's torque is evenly distributed and does not cause rotation around the adverse axis. Their profile increases the drag due to freefall and reduces air resistance associated with rotatory movement. The inserted carbon rods will provide additional strength. In the rocket, the rotor blades will be locked in special pockets **(Figure 2)**.

The airflow around the CanSat will push the blades upwards. The rotating movement will give rise to a centrifugal force, which will keep them open. The mount system transfers air drag

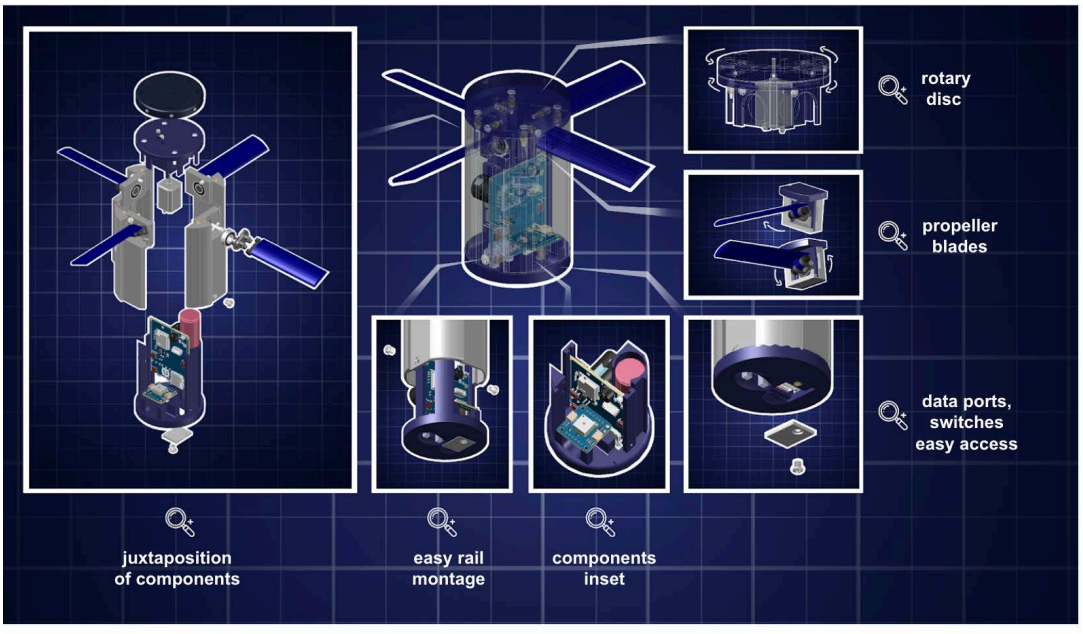

Figure 2 – Selected case features

forces to the main body. It contains a hinge reinforced with a metal rod **(Figure 3)** placing the wing in the correct position.

Another important factor is that blades must be angled to generate torque on the vertical axis. Considering freefall drag torque accelerating the blades and rotary air resistance, the most efficient attack angle is 65º-75º. The hinge, which sets the blade into the final position, has been placed on the platform **(Figure 3)**. It will be able to rotate in the range limited by the channels in the case. Rotation on the platform will cause the blade to tilt around its length, which will set the attack angle. This movement will be induced by air drag on the blade. Through the blades' mounting point drag force is transmitted. Additional torque will be generated by the rotatory parachute, from which rotational momentum will be transferred to the electric generator. However, there is a danger that the strings, which transfer the force, will twist.

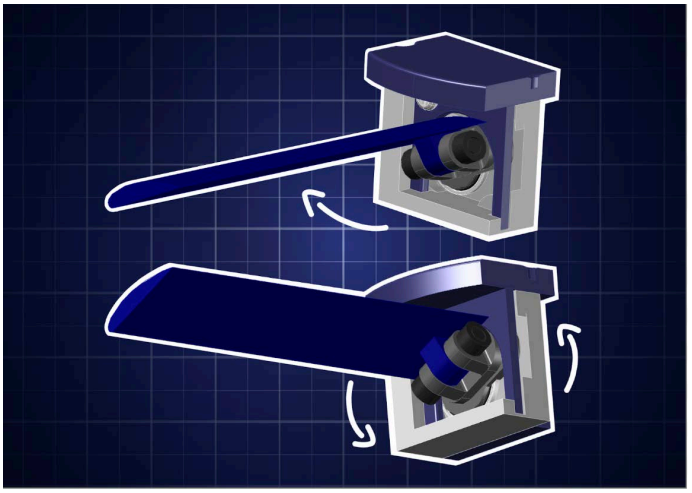

Figure 3 – Render of the blades and mount

To avoid this effect the generator's shaft has been connected to the rotary disk **(Figure 4)** and instead of standard strings, braided steel ones are used. They are much less prone to entanglement due to their springiness. On its circumference, the parachute's strings have been mounted on swivels, which increases the torque necessary to tangle the parachute. The rotary disk has a spot where the magnet can be fitted snug enabling detection of rotation speed by a Hall effect sensor. When in the rocket, the parachute will be folded and stored on top of the disk, in such a way that after escaping the socket it will open automatically due to the airflow. The theoretical maximum rotational speed for the main body of the CanSat is estimated to be **5880 revolutions per minute** from the equilibrium of air drag torque caused by freefall and the rotational movement of the blades, though the real value will be much lower due to interior resistance and airflow at high speeds, both of which will create centrifugal force, which will be applied to every component.

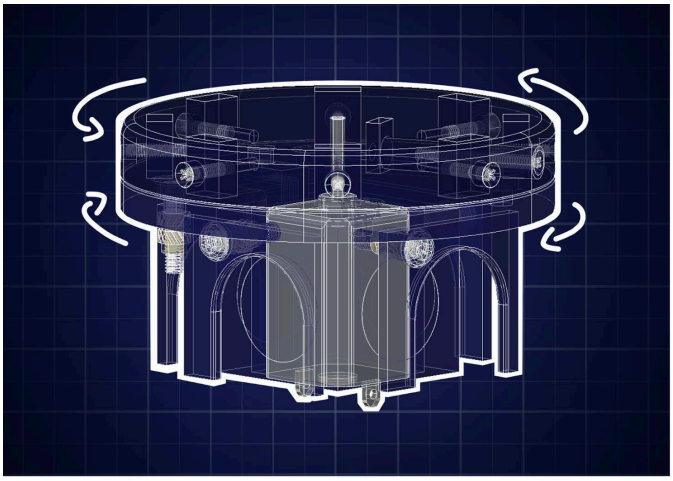

Figure 4 - Rotatory disc

The main component has been 3D printed out of **Polycarbonate,** which has high tensile strength. This is paramount in this project, as the satellite will be rotating quickly. To facilitate a quicker printing time and easier assembly process, the model has been split into multiple parts. The PCB has been mounted on special rails for easy access. It will be able to slide out of the rails after opening the satellite lid in its lower end (**Figure 5** - in the middle). Additionally a special holder for the battery allows attaching a disc made of sponge to cushion the vibrations (**Figure 5** - on the right). Other features include: a pocket-shaped cover designed specifically to protect the USB port from dirt or water intrusion as well as an SD card port cover (**Figure 5** - on the left).

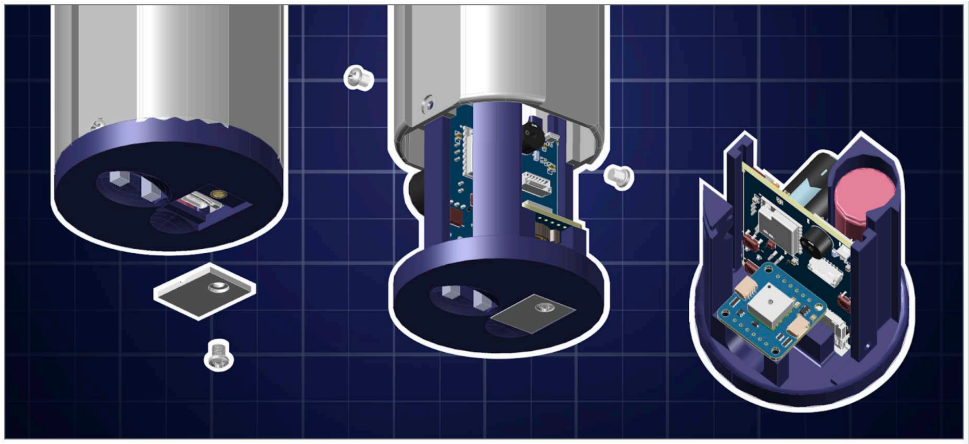

Figure 5 – Bottom protection and inertial part holder

Link to higher quality renders, Link to an interactive 3D model

3.3 Electrical Design

General Architecture

The electrical system of the CanSat was designed with reliability, safety, and ease of manufacturing as the main priorities. The schematic shown in **Figures 7** and **8** was specifically created with the PCB conversion in mind. Most of the components, including the microcontroller, are SMD making the PCB very compact. The availability of used components was checked in the manufacturer's part library. This way a professionally-made, clean end product with no unnecessary cables prone to tangling or failures could have been manufactured.

A single **18650 Li-Ion battery** acts as a power supply to the satellite. It can provide high

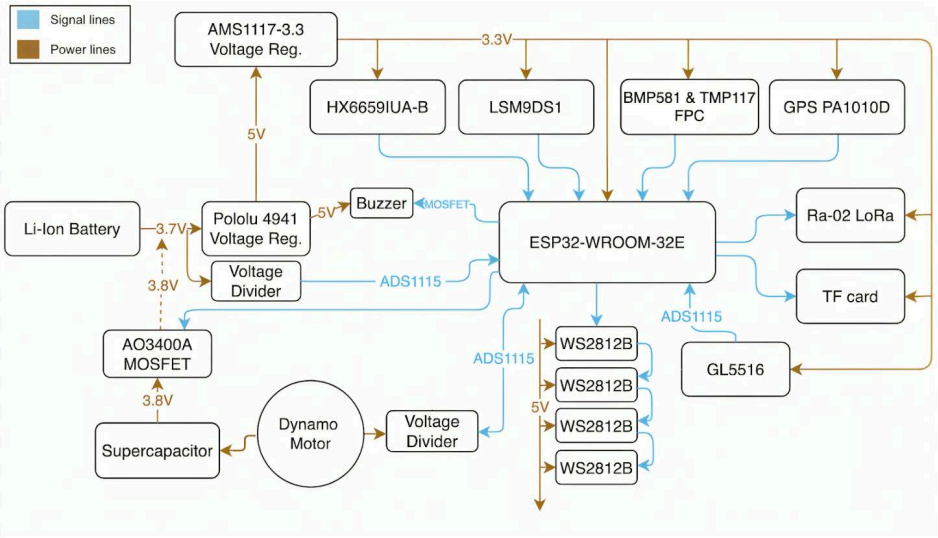

Figure 6 – Simplified electrical schematic

energy density and has a proper size to fit into the CanSat. Its voltage is stepped up to 5V using the **Pololu 4941** which is more than capable of providing enough current to power the rest of the components. The voltage is also stepped down with **AMS1117 3.3V** powering lower voltage components including the **ESP32-WROOM-32E** microcontroller.

ESP32-WROOM-32E is an advanced model of the popular ESP32 family. Coming with a dual-core 32-bit LX6 processor it is highly capable of handling multiple complex tasks. It has powerful and numerous peripherals with many interfaces such as SPI, I2C, UART, PWM, ADC, and DAC, with a USB-C connection added for easy programming and high-speed data transfer. This makes it ideal for interfacing with sensors and other hardware onboard the CanSat. It has **WiFi** capabilities which allows for running a ground station LAN website with retrieved data. Furthermore, it comes at a very attractive price point. Nevertheless, one of the drawbacks of this microcontroller is its poor Analog to Digital conversions which are often found do be non-linear, to solve this issue the **ADS1115IDGSR** analog to digital converter was added, to get more accurate data from both voltage dividers and the **GL5516** photoresistor, used to determine when the CanSat exits the rocket.

Optional connector solder pads have been added so that it would be possible to access the pins of the ESP32 in case of any errors or troubleshooting. On the simplified schematic presented in **Figure 6** all of the devices have been added. Red arrows represent power lines, blue lines signify signal lines, arrows show the direction of information/electricity flow. A zoomable, updated version of the full **schematic can be viewed** here.

Primary Mission Devices

The primary mission will be carried out by three key components: a temperature and pressure sensing system, a LoRa radio module, and a microSD card housed in a dedicated socket (**Figure 7**).

For pressure and altitude measurements, the **BMP581** sensor was selected due to its proven reliability and cost-effectiveness. This sensor enables accurate altitude determination, ensuring precise environmental monitoring throughout the mission. For temperature measurements, the **TMP117** was chosen for its high precision and I²C interface.

Both the **BMP581** and **TMP117** replace the previously used **BME280** sensor. To accommodate this change, a **flexible PCB** was implemented. It is soldered in place of the original sensor, with the new components mounted on it. This design allows the **temperature sensor** to be positioned **outside** the CanSat for more representative ambient readings, while the pressure sensor remains shielded from wind, significantly improving measurement stability.

In addition to improved sensor placement, both the **BMP581** and **TMP117** offer significantly greater accuracy than the BME280. For example, the BMP581 provides a pressure accuracy of **±0.06hPa** compared to the BME280's **±1hPa**, while the **TMP117** achieves a temperature accuracy of **±0.1°C**, substantially outperforming the **BME280's ±0.5°C**.

The **LoRa** communication system was chosen for the CanSat mission due to its exceptional range, reliability, and efficiency, particularly for long-distance transmissions. Radio communication is a crucial element not only for the primary mission but also for secondary mission objectives and the recovery system. To facilitate communication between the ground station and the probe, two **Ra-02 LoRa 433MHz** radio modules will be utilized — one in the CanSat itself and the other one at the ground station.

This configuration was selected because it balances high range, reliability, and cost-effectiveness when compared to other communication systems. The LoRa modules will handle all data transmission between the probe and the ground station, ensuring robust and fast communication even over significant distances. To ensure that the CanSat can be reliably located after deployment, the **GPS PA1010D** module has been selected. This GPS module is known for its high sensitivity and low power consumption, making it ideal for space-constrained projects like this one. It has a position accuracy of 2-4 meters, which is more than sufficient for tracking the CanSat's location during the mission. It also allows for reliable I^2C communication.

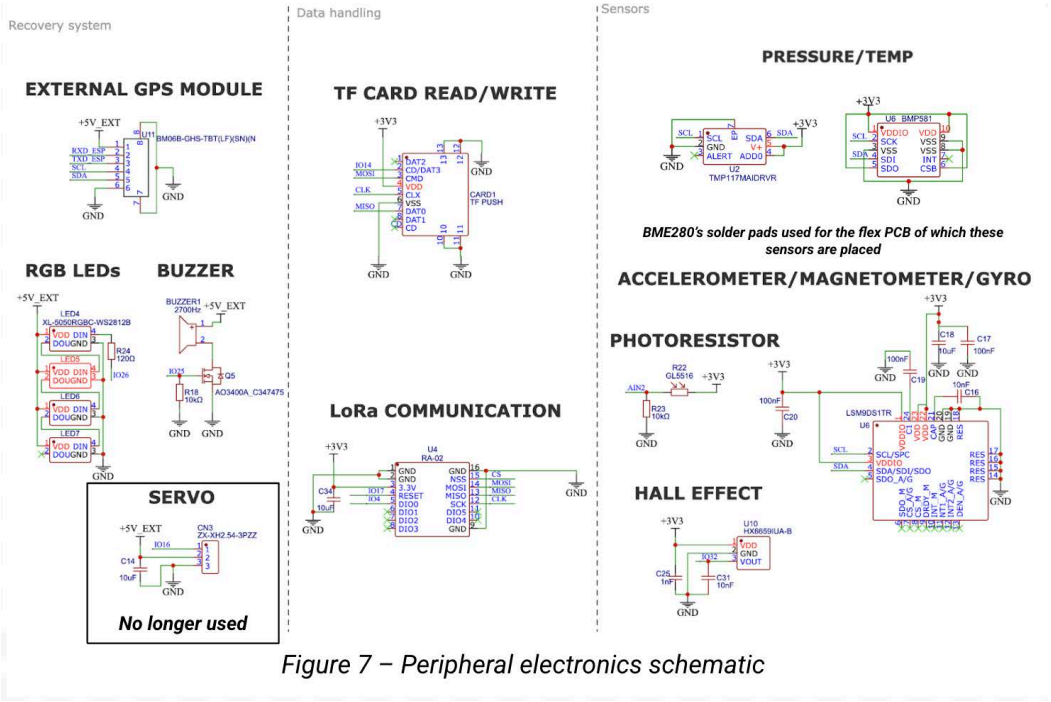

Figure 7 – Peripheral electronics schematic

Secondary Mission Devices

The secondary mission revolves around managing and examining the performance of the dynamo motor. A **24V PMDC motor** is used as a dynamo. The current generated by the dynamo will be pushed through a **Schottky diode** (**Figure 8**) to prevent reverse current flow and protect the system from potential damage.

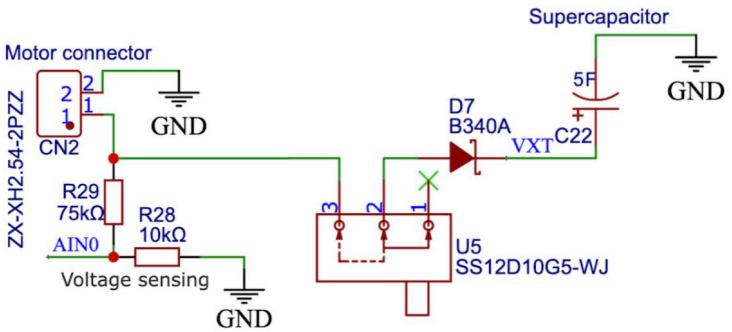

Figure 8 – Supercapacitor electronics diagram

A simple voltage divider (**Figure 8**) has been integrated into the design to measure the motor's output voltage, ensuring accurate monitoring during operation. Additionally, a 9-axis accelerometer, magnetometer, and gyroscope module will track the position and rotations of the CanSat, providing valuable data on the energy harvesting system's performance. A **HX6659IUA-B** Hall effect sensor will measure the time at which the magnet mounted in the rotary disk is rotating relative to the main body of the satellite. This data will be analyzed to assess how efficiently the dynamo converts motion into electrical energy. After the CanSat reaches the ground, the capacitor charging will be deactivated with a switch, and the energy stored in the supercapacitor will be checked using a simple circuit consisting of a resistor, voltmeter and ampere meter to verify its effectiveness. The option of software-induced power switching is available, which makes it possible to use the capacitor's stored voltage upon landing.

Power Supply

Before selecting a power supply for the satellite, the power consumption data of each component was collected from their respective datasheets. The total power requirements were calculated and are presented in **Table 1**. The efficiency of the step-up and step-down converters was also taken into account, typically ranging between 85–90%. These losses were included in the power budget to ensure a realistic estimation of battery life under actual operating conditions.

A single **18650 Li-Ion battery** was chosen due to its compact cylindrical form factor, which fits well within the satellite's mechanical constraints. The battery offers a high energy density and a capacity of **3500 mAh** at a nominal voltage of 3.7 V. To enhance system reliability, the battery voltage can be monitored through a voltage divider. The voltage is regulated via step-up and step-down converters (**Figure 6**) to provide the necessary 5 V and 3.3 V rails required by the onboard electronics. Additionally, decoupling capacitors have been strategically placed near the most critical components to ensure uninterrupted operation during transient current spikes. The max voltage when fully charged is equal to $V_{Fc} = 4.2V$. The cutoff voltage of the step-up converter is $V_{Co} = 1.9V$. Working time can be estimated from the following formula where t is the battery lifetime, Q is the battery capacity and P is the CanSat's power consumption:

$$t = \frac{Q \cdot \frac{V_{Fc}+V_{Co}}{2}}{P}$$

Taking into account the converter losses, the total **working time** of CanSat was estimated to be **405.6 minutes** (6.76 hours**)**. As the buzzer is not turned on for the entire duration of the mission, the battery lifetime excluding it was estimated to be **421 minutes**. The satellite system has been designed with energy efficiency in mind. Owing to its low power consumption, a single 18650 battery provides sufficient energy reserves. The calculated runtime of over 6.5 hours (under realistic conditions) significantly exceeds the mission duration of 5 minutes, including the time needed for recovery operations. Therefore, one battery is more than adequate for the mission requirements.

Name	Voltage (V)	Current (mA)	Power (W)	Power adjusted by converter efficiency
ESP32-WROOM-32E (no WiFi)	3,3	50	0,17	0,252
Ra-02 LoRa module	3,3	120	0,4	0,593
PA1010D GPS module	3,3	28	0,09	0,133
LSM9DS1TR accelerometer, magnetometer, gyroscope	3,3	10	0,03	0,044
HX6659IUA-B hall effect sensor	3,3	4	0,013	0,019
4x WS2812B RGB diodes constantly on (blue 255)	5	80	0,4	0,444
Photoresistor	3,3	1	0,003	0,004
BMP581 pressure sensor	3,3	1,8	0,006	0,009
TMP117 temperature sensor	3,3	10µA	0,00003	0,00004
ADS1115 ADC	3,3	0,15	0,0005	0,001
microSD module	3,3	5	0,017	0,025
Buzzer (turned on after landing)	5	10	0,05	0,056
Total:			1,17953	1,581

Table 1 – Energy consumption of parts

Generated Power Storage

The capacity of the used supercapacitor can be chosen by optimizing it to captivate maximum amount of energy. The way the team found the optimal capacity for the supercapacitor for the project is described below:

Starting with the voltage across the capacitor over time during the charging, it can be calculated using the following equation for the RC circuit:

$$U(t) = U_0(1 - e^{-\frac{t}{RC}})$$

where: $U(t)$ - voltage across the capacitor over time t , U_0 - desired voltage (which the capacitor is trying to reach) C - capacitor's capacity, R - circuit resistance

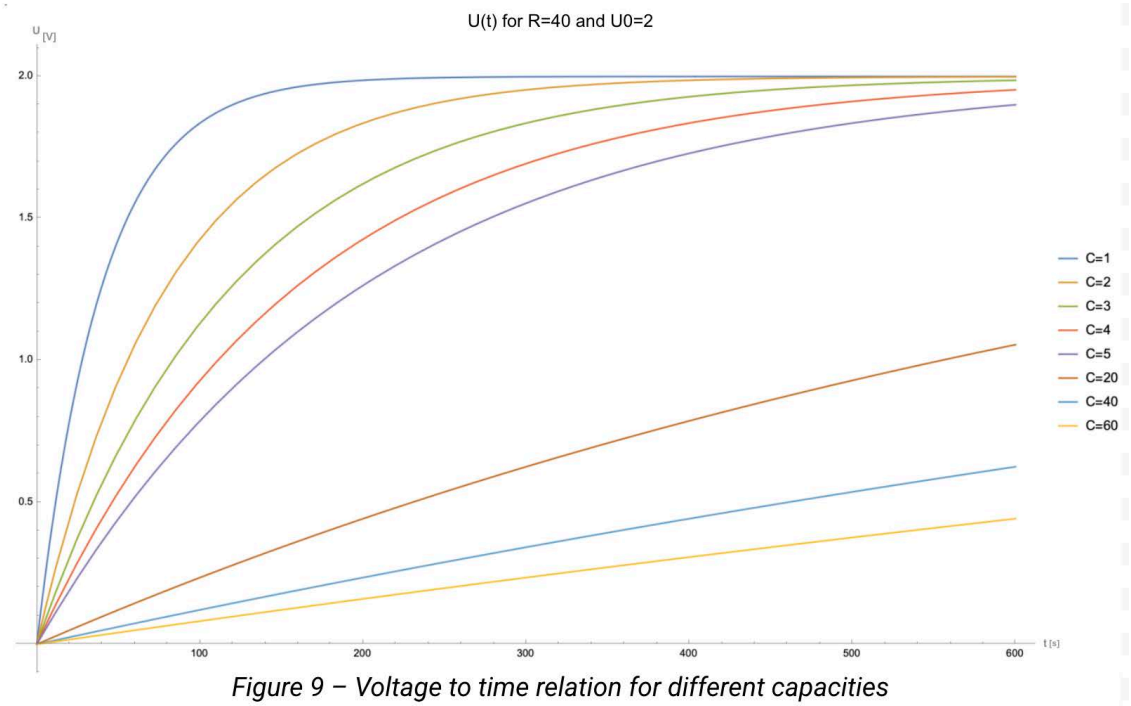

Figure 9 – Voltage to time relation for different capacities

The voltage on the capacitor during charging for different capacities in farads has been presented in **Figure 9**. The resistance of the motor circuit was estimated to be 40Ω during tests, which is the standard solution for RC circuits. It may be observed that capacitors with lower capacities achieve 2.0V faster than the ones with higher capacities. While this is a sensible finding, it is not a significant enough indicator in choosing the right capacity. The most important aspect is the energy possible to collect. That energy may be calculated in the following way:

$$E = \frac{1}{2}CU^2(t) = \frac{1}{2}CU_0^2(1 - e^{-\frac{t}{RC}})^2$$

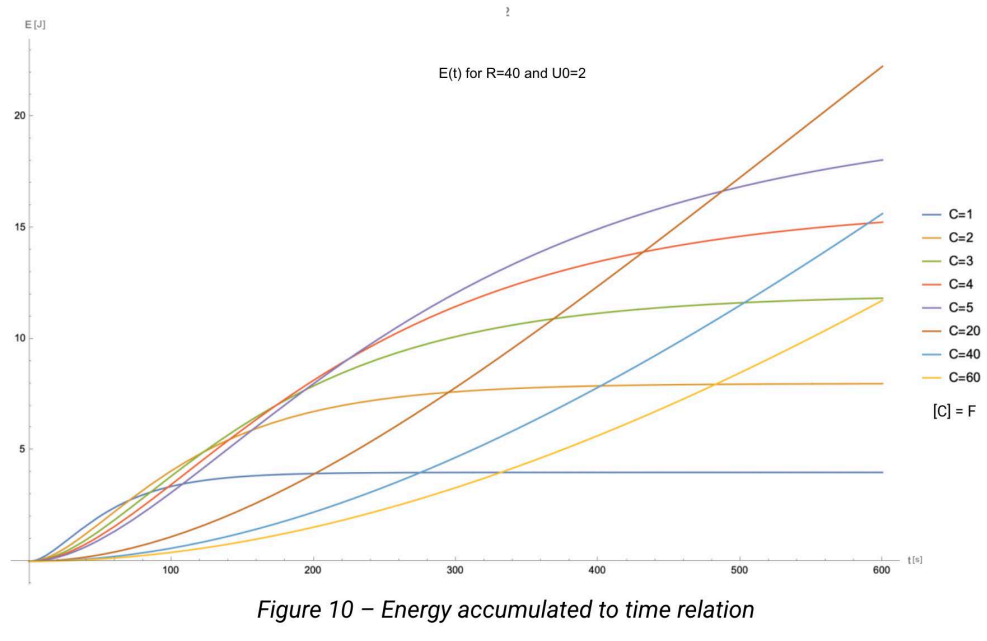

Figure 10 – Energy accumulated to time relation

Figure 10 shows the amount of stored energy in the capacitor for each tested capacity. For times between 100s and 200s energy values are similar for C=3F, C=4F and C=5F. If the satellite descended from 2000m, with 8m/s as its descent rate, it is expected that it will take 250s for it to land. That is why the **PHB-5R0V505-R** supercapacitor with the **capacity of 5F** was chosen. Starting from roughly 220s, that capacity is the most optimal for the mission. It is estimated that at 2.0V around 6-12J of energy will be collected. That energy could be used for:

- Power supply of the temperature and pressure sensors for:
  - ~11 minutes for 6J of energy stored,
  - ~22 minutes for 12J of energy stored,

  Or
- Power supply of the microSD module enabling to store data for:
  - ~4 minutes for 6J,
  - ~8 minutes for 12J,

That means **the energy** collected from this mission would be sufficient either to power **the primary mission** sensors or to store data on **the microSD** module for a mission of the same duration.

Communication System

In the purpose of minimizing the power consumption due to the communication system, the most efficient solution is one-way transmission from the CanSat to the Ground Station. As it was mentioned, communication uses the LoRa standard, which is the best choice in this case. It provides long-range and stable radio data transmission with low power consumption. The onboard radio transmitter and Ground Station's receiver will both be **LoRa Ra-02 SX1278** modules to eliminate potential conflicts. The ground radio set also includes a **directional ATK-10 antenna**, which will be aligned with the CanSat by team members. The CanSat's main body contains a small flexible **Molex 204287-0050** antenna due to the limited space. The transmitter will send a data pack every second, which will be received by the Ground Station if both antennas are positioned correctly. The ground station computer is the same as the CanSat's, as there are some spares left. This allows for a clean and error-free setup.

Both communication systems are designed to operate within **ISM 433MHz radio band**; also the **bandwidth is set to 125kHz**, being the highest acceptable value. In order to enhance the range of stable transmission, the **perimeter of the spreading factor is 8**, as this value provides suitable throughput, changed from the default value of 7. During the test, where both antennas were put in the closest distance possible (about 10cm) and the **maximal signal strength was -27dBm**, which considering the losses due to the separation and receiver resistance cannot surpass the maximum strength of 20dBm set by the competition rules.

3.4 Software Design

Onboard Software

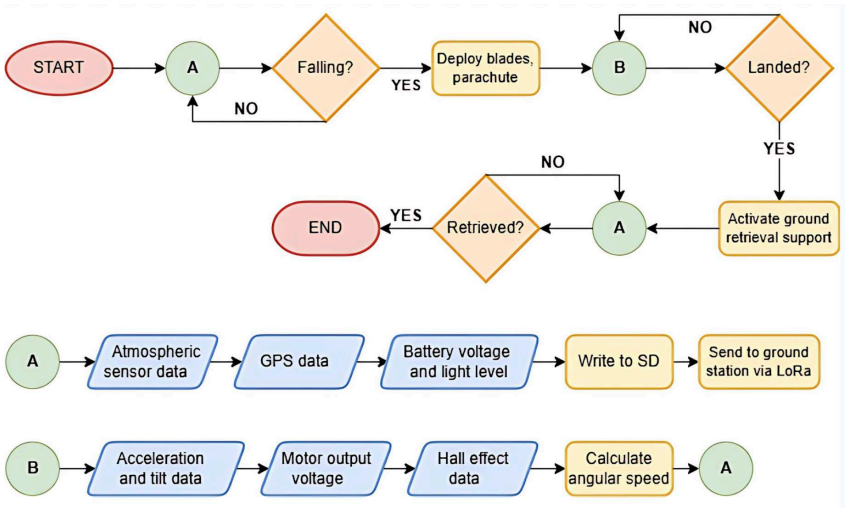

Figure 11 – Flowchart presenting the simplified onboard program flow

The onboard software operates on the **ESP32-WROOM-32E** microcontroller, serving as a central computer for the CanSat. The program has two data-collection states: low-power consumption (**A** in **Figure 11**) and normal mode (**B** in **Figure 11**). The former will be active in the rocket and after landing and will preserve basic functions to reduce battery consumption. Once the program detects a non-negligible drop in altitude and a sufficient light level, it will switch into normal mode. After landing, an additional ground retrieval support system, consisting of visual and auditory signals, will be activated and will remain active until the CanSat is switched off.

The low-power consumption mode will be active until the CanSat begins its descent. During its operation, atmospheric, location, battery voltage, and light level data is collected from the sensors colored blue in **Figure 12**, including: the **GL5516** and **Battery Voltage Divider** via the **ADS1115IDGSR**, as well as the **BMP581**, **TMP117**, and **PA1010D** sensors. Once the program switches into normal mode, additional data will start being collected from the sensors marked in red in **Figure 12**, including: the **Motor Output Voltage Divider** via the **ADS1115IDGSR**, as well as the **LSM9DS1**, and **HX6659IUA-B**, using which the relative angular velocity between the parachute and body is calculated, by detecting peaks in the Hall effect sensor output when the magnet in the rotary disk nears the sensor**.** The acceleration, tilt, energy generation data, and rotational speed is packaged together with the rest of the sensor output, saved on a **micro-SD card,** and transmitted to the ground station via **LoRa** (purple in **Figure 12**).

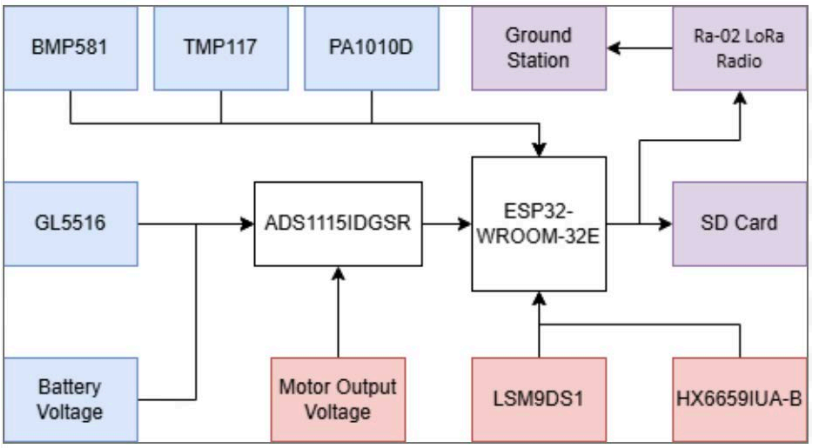

Figure 12 – Diagram showing the data handling onboard

To estimate the amount of data gathered a series of assumptions must be made. First of all, the total runtime of the program has to be estimated, as well as the time that it will be in low-power versus normal mode. The maximum total mission time will be 216000s (6h) and for 300s (5min) the CanSat will be in normal mode. The total SD data package size can be calculated to be **around 120B**, this comes from the fact that the data is saved as a semicolon separated string. Now, using the target 1Hz refresh rate for all the sensors, and ignoring the fact that the normal mode components will only be active for 300s out of the total 216000s, the total amount of data gathered on the SD-card will be roughly equal to **26MB**. It is important to note that this number is an estimate, nevertheless, it confirms that the chosen 2GB micro-SD card will be **entirely sufficient**. The size of the packets transmitted via LoRa is smaller, being equal to **roughly 85B**. This was achieved by not transmitting some redundant information, instead opting to only save it on the SD-card or reconstruct it at the ground station.

Ground Station

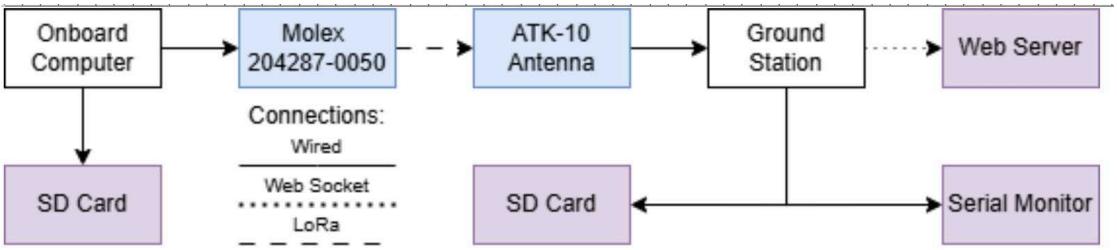

Figure 13 – Data transfers between the ground station and CanSat

Figure 13 fully describes the final data outputs (in purple) as well as the connections between them. The data gathered by the onboard computer will be saved on a SD-card before being sent via LoRa communication (in blue) to the base camp. Upon its arrival at the ground station it will be: displayed on the serial monitor for quick insight into the data stream, saved on a second SD-card to ensure reliability and check connection quality, and transmitted via a web socket connection to a locally hosted web server, which will display a live dashboard. Choosing this multi-faceted approach ensures that data will not be lost in case of subsystem failure.

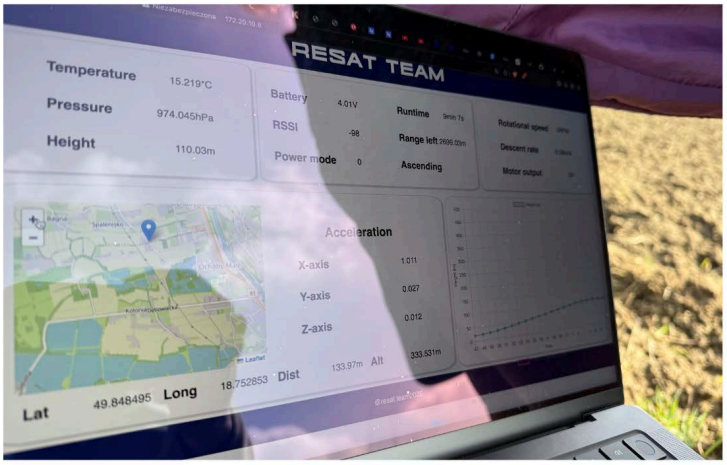

Figure 14 – Photo of the live web server dashboard

The live dashboard is visible in **Figure 14**. It has been split into 5 distinct parts, displaying: primary and secondary mission data, the signal strength, location and distance of the CanSat, as well as two dynamic plots of altitude against time and motor output voltage against rotational frequency. Furthermore a live map view with the current location of the CanSat has been added for easier localisation after touchdown. Through this interactive, high-speed interface the team will be able to easily monitor the mission progress.

Development Environment

The onboard software was programmed in **C++** using any necessary APIs to make interacting with the sensors easier in the **Arduino Integrated Development Environment**. The ground station's microcontroller code was written in the same environment. The web server was coded using the HyperText Markup Language (HTML5), Cascading Style Sheets (CSS), and Javascript (JS) with the addition of Leaflet.js (used to embed a live map) and Chart.js (used to create dynamic real-time graphs). The web server files were ported to the ground station microcontroller via Little FS and stored there for quicker data processing. While developing the software the Git version control system was used and all of the progress is visible on GitHub.

3.5 Recovery System

The parachute not only fulfills its mandatory objectives but also helps with the secondary mission because of the asymmetricity of its design. The material that was used for that matter is a bright yellow **ripstop 40D nylon**, owing to its exceptional strength-to-weight ratio, hence wide use in the parachute industry and vibrant color, which will make the recovery process easier.

Parachute Design

The design is different from that of a standard CanSat parachute, making it rotate so that mechanical energy can be taken in and converted into electrical energy. This type of parachute is

called a **rotafoil**, and the single gore can be seen in **Figure 15b**. The asymmetry of the gores results in the parachute's rotational motion.

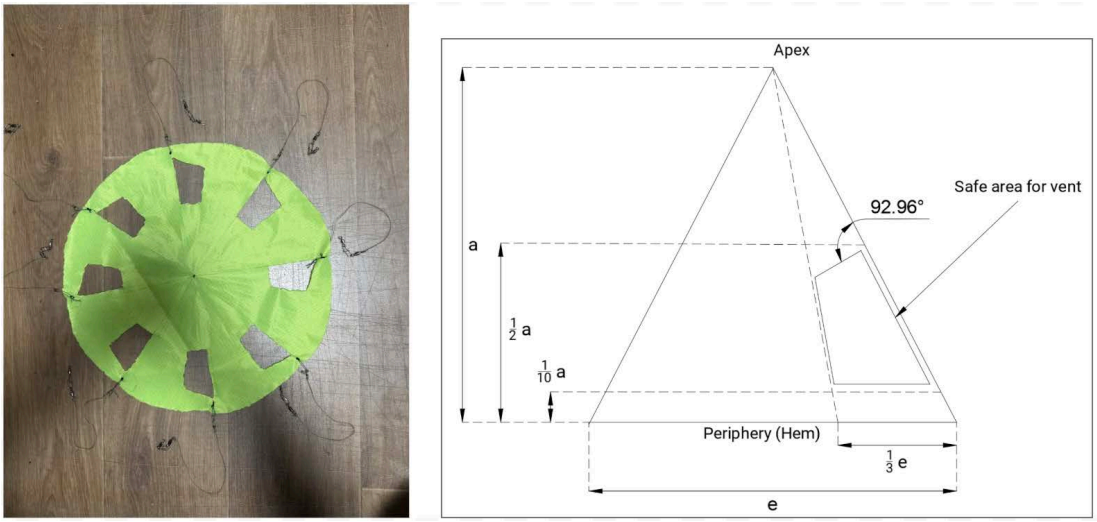

Figure 15 – Photo of the parachute (a) and gore design (b) (source)

The effect is enhanced thanks to the accurate placement of the vents, and the ratios in the single gore. It rotates in the opposite direction of the CanSat's body and blades. The current version of the parachute is displayed in **Figure 15a**.

Mounting system

The thin (0.3mm), **steel ropes** are attached to the rotary disk at the top of the satellite. This disk is connected to the motor shaft (**Figure 16**), causing it to spin together with the rotafoil. The choice of steel was determined by the need for the wire links not to twist during the rotational motion of the parachute. The rotafoil will be folded and placed into a special place at the top of the CanSat. Since the ropes are thin, it is possible to bend them while folding. When the CanSat exits the rocket, the paracords will straighten out thanks to their physical properties. Additionally, the use of **swivels** and **snaps** facilitates quick and efficient replacement of paracords during testing or tanglement. These components are well-suited for attaching fishing leaders, which serve as an ideal option for paracords due to their precise length and ease of installation.

Figure 16 – Mounting of the paracords to the rotary disk

Estimated Performance

m - mass (350g), g - gravitational acceleration - $9.81\frac{m}{s^2}$, C_d - drag coefficient (taking into account the rotational motion, roughly 1.2), ρ - density of air, A - area of parachute, v - descent velocity

$$mg = \frac{1}{2}C_d \rho A v^2$$

$$A_{min} = \frac{2mg}{v_{max}^2 \rho C_d} = 0.0475m^2, A_{max} = \frac{2mg}{v_{min}^2 \rho C_d} = 0.190m^2$$

Due to irregular design, the drag coefficient is difficult to estimate. Moreover, the blades' influence will also cause the air resistance to be greater. The area after the simulation was established to be ~**0.09**m^2 (area of a circle without the vents) with a **radius of 18cm**. This has allowed the satellite to achieve average descent velocities varying between **5-8m/s.** After testing the dimensions remained the same, since everything was in order.

GPS Module

The GPS module is crucial in the recovery process. That is why the GPS **PA1010D** module, described further in Section 3.3, has been chosen. When it comes to recovery, the accuracy of the tracking of the device is the most significant factor in choosing the right module and the one that has been chosen fulfills this aspect perfectly. It is equipped with a RTC slot for a CR1220 which enables fast startup, thus making the starting campaign much easier and enabling quick hot starts in case any errors occur midair.

Parachute 3D Model

The 3D model of the parachute, shown in **Figure 17**, was essential for the **CFD** simulations discussed in Section 4.5. Additionally, it streamlined the sewing process by providing precise dimensions. The model was created using **SolidWorks**, with a free subscription generously provided by the company for the project. The rotary disk at the bottom illustrates how the parachute's rotational motion is used to generate energy. The ropes connect to the disk, which is mounted on the motor shaft, enabling it to spin and produce electrical energy, in turn charging the supercapacitor.

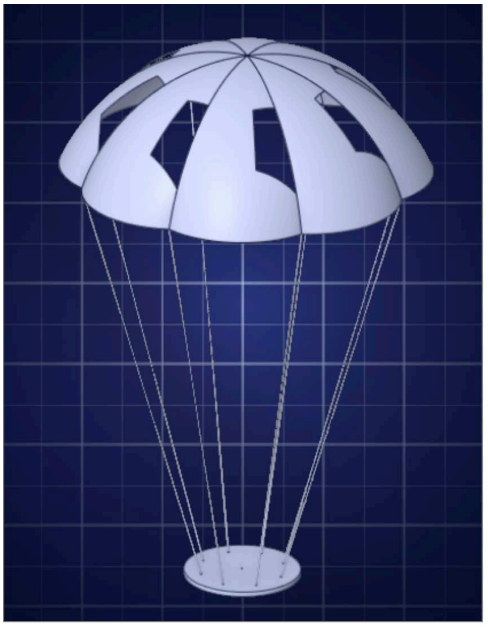

Figure 17 – Parachute 3D model

3.6 Ground Support Equipment

In order to complete both missions, the ground support equipment consists of the a spare PCB (including the **Ra-02 SX1278 LoRa** radio receiver and an **ESP32** board), a **ATK-10/400-470 MHz** antenna, and a laptop, which will decode data packs and make basic live analysis. Moreover, it will track the altitude and GPS location which are crucial in the successful recovery of the CanSat.

For the radio receiver the same PCB as the one onboard CanSat will be used. The signal from the CanSat will be received by the **directional ATK-10 antenna (Figure 19)** operated on an

azimuthal montage (**Figure 18**) by team members. This model has been chosen because of its high range, simple construction, and high targeting precision, which minimize the margin of reading error and the risk of disconnection due to imperfect alignment. The raw signal will be transmitted with the **SL16** wire to the **SX1278** radio on the PCB. The received data will be visible on the **web server hosted** from the microcontroller connected to one of the team members hotspot and logged in the serial monitor.

If the connection remains in sufficient condition, every second the Ground Station will receive data regarding the outside temperature, and air pressure inside the CanSat, GPS location (including longitude, latitude, and altitude), light level, acceleration, voltage on the generator and battery to ensure that the secondary mission works well, as well as angular speed calculated using the **Hall effect** sensor. Moreover, the current position and trajectory will be displayed on a map to support tracking the CanSat in the case of restricted visibility and recovery process. Furthermore, live charts will be created to provide better insight into the progress of the primary and secondary missions. Transmitted data will be saved on a secondary **SD card** as a **CSV file**, which can later be compared with the CSV file from the CanSat's micro-SD card to check in case any package loss occurred. This also allows for analysis of the signal strength throughout the mission as the **RSSI** values will be saved.

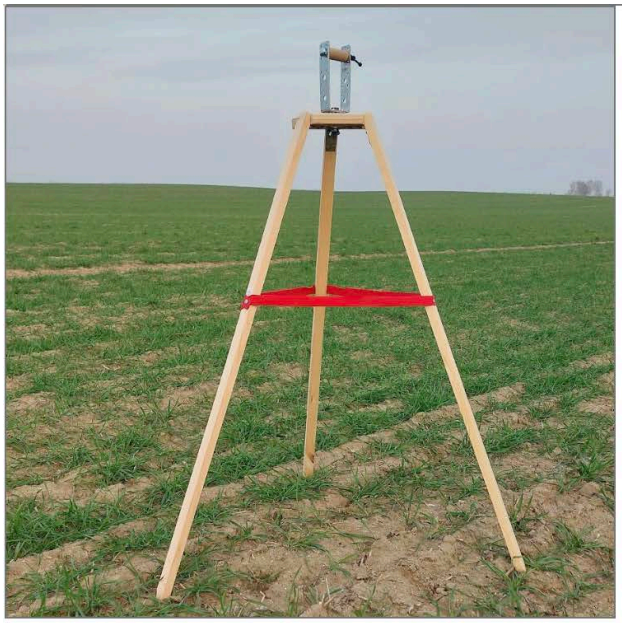

Figure 18 – Azimuthal montage

Figure 19 – ATK-10 directional antenna

4 Test Campaign

4.1 PCB Post Production Tests

Upon receiving the PCB **(Figure 20)** from the factory a set of tests have been conducted to ensure proper functioning and no manufacturing details. The team has gone through the following checklist:

- ☑ Code uploads to the ESP32 properly
- ☑ The built in user LED works
- ☑ Photoresistor returns correct values
- ☑ A/D converter works returning accurate values
- ☑ Buzzer can be switched both ON and OFF
- ☑ RGB diodes light up, addressability can be used
- ☑ Accelerometer/magnetometer/gyroscope returns correct values
- ☑ Thermometer, barometer and hygrometer return correct values
- ☑ SD card reading and writing works flawlessly
- ☑ Hall effect sensor detects magnetic field
- ☑ GPS connects to satellites and returns correct position and altitude
- ☑ Motor voltage sensing returns correct values
- ☑ LoRa communicates with the second module
- ☑ Power source switching
- ☑ Supercapacitor charges
- ☑ PCB can be powered from battery, voltage converter works properly
- ☑ No I^2C address conflict occur
- ☑ The flexible PCB solders securely to the main PCB pressure and temperature sensors work properly

In conclusion, all of the components of the PCB work flawlessly except the GPS module which used the USB Serial's UART port which made it impossible to retrieve any data from it. However, this was a quick fix, swapping it for a one just as capable but with I^2C communication protocol available.

Multiple flex PCBs were ordered for different pressure sensors to choose the most accurate one.

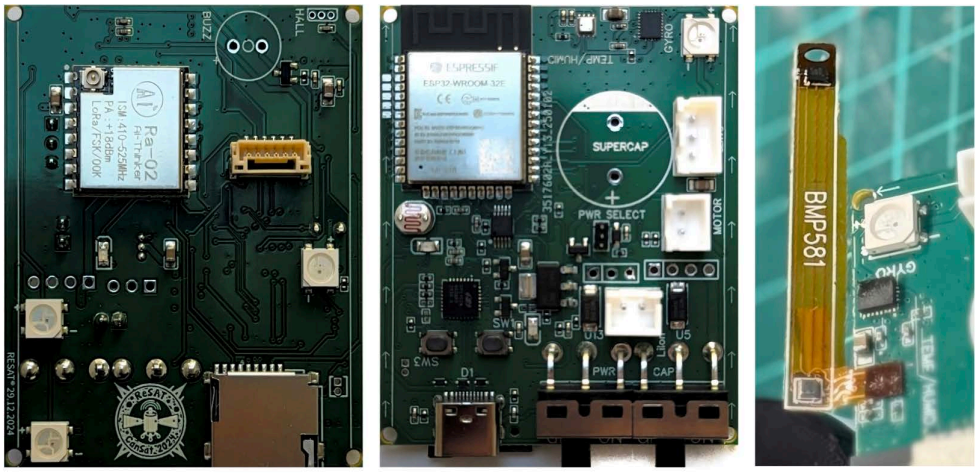

Figure 20 – Pictures of both sides (a),(b) of PCB board and flexible PCB (c)

4.2 Primary Mission Tests

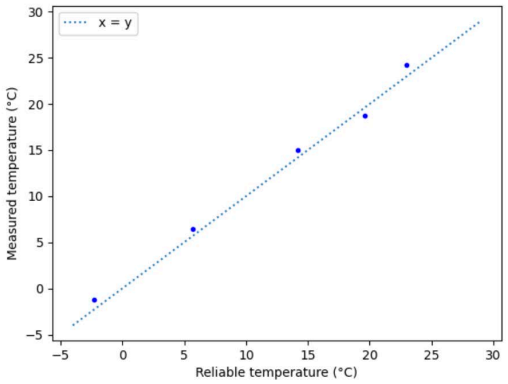

Figure 21 – Graph of temperature against temperature

To measure the reliability of the temperature sensor, a series of measurements was conducted and later referenced to a reliable thermometer in **Figure 21.** The resulting data points are quite close to the expected readings, certainly within the combined measurement uncertainty of both sensors. The results prove that the TMP117 is more accurate than the previously used BME280. After conducting the static temperature tests to ensure that the TMP117 is capable of providing accurate readings, temperature data was also collected during the plane drop test, to test its dynamic temperature measurement capabilities.

The results of this test have been displayed in **Figure 22** as a graph of relative altitude and temperature against time. For the first 8 seconds the CanSat was inside the plane, where the temperature was measured to be around 19.5°C by an independent thermometer, the temperature measured by the CanSat was almost identical. In the 9th second the CanSat was held outside of the airplane until the 14th second, when it was released and started its descent. On the day of the drop test the outside temperature measured by a nearby meteorological station was 11.8°C, the slightly higher readings during the fall are likely due to heat being generated by the drag forces. Overall, it can be said that the temperature sensor provides highly responsive and accurate output.

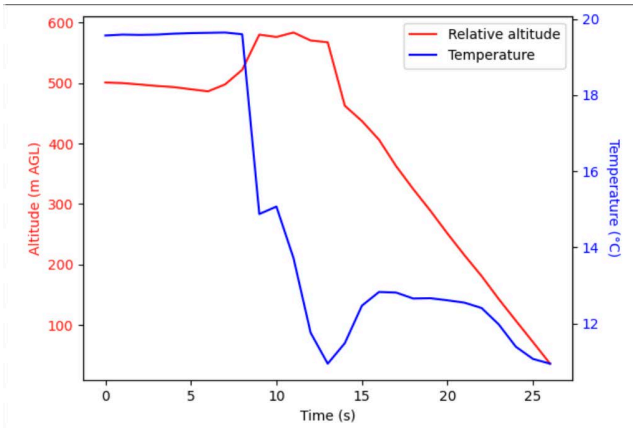

Figure 22 – Temperature and relative altitude against time from plane test

To ensure that the pressure readings from the BMP581 are correct, during a drone drop test, the recorded GPS altitudes and pressure values were collected. Using the barometric formula the altitude in meters above mean sea level was calculated. This revealed that the pressure sensor was miscalibrated, which was fixed by measuring the accurate altitude at ground level and applying a correction factor to the altitude calculated from the pressure. In **Figure 23** it is evident that from the moment that the GPS started returning altitude readings to around 200s both the sensors are in

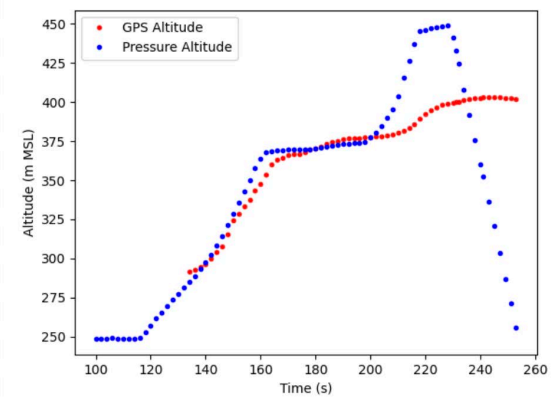

Figure 23 – Graph of the altitude from GPS and pressure against time

sync. The differences after 200s can be easily explained by the fact that the pressure altitude is significantly more responsive, since it is visible that both during the second ascent period and during the descent period the GPS altitude readings started moving in the same direction as the pressure altitude readings simply slightly later and at a lower rate of change. Therefore, during the launch campaign the elevation will be calculated from the pressure readings for full responsiveness and referenced to the GPS altitude at the ground station. Comparing the results with the fact that the test was conducted in Ochaby, where the average elevation above sea level is 260 meters and that right before the drop the drone altimeter read roughly 200 meters, the conclusion may be drawn that the pressure sensor after calibration is surprisingly accurate and conveys an accurate picture of reality. Hence, both the TMP117 and BMP581 will **fulfill the primary mission** requirements with no problems.

4.3 Secondary Mission Tests

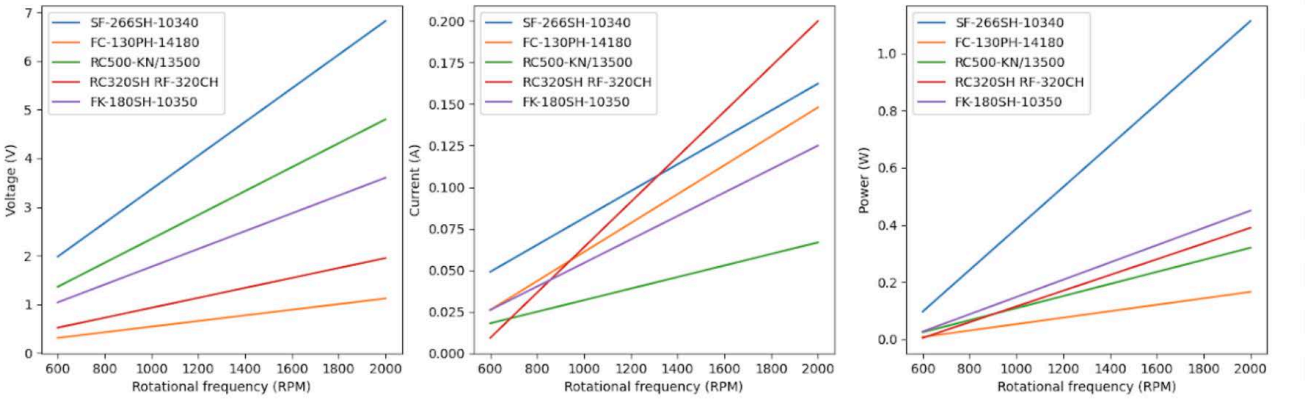

Figure 24 – Graphs of voltage (a), current (b), power (c) against rotational frequency of 5 dynamos

A total of five motors were evaluated using a specialized testing rig. The setup consisted of a dynamo motor connected via its shaft to an electric screwdriver with an adjustable rotational speed. A magnet was fixed to the adapter linking the motor shaft to the screwdriver, and a linear Hall effect sensor, connected to the PCB, was used to measure the time intervals between high-value peaks. This configuration enabled the collection of precise data, which was subsequently plotted in a linear format to clearly illustrate the results in **Figure 24**. Even though the RC320SH RF-320CH was capable of producing a higher current at high rotational frequencies (**Figure 24b**), the **SF-266SH-10340** motor clearly dominated in terms of voltage produced (**Figure 24a**) and total power output (**Figure 24c**), making it the optimal choice for the secondary mission.

After selecting the proper dynamo, more complex tests were carried out. The rotational dynamics of the CanSat relative to its parachute were assessed through a controlled drop test. The satellite was dropped from a building at an altitude of **5 meters**. High-frame-rate video recordings were captured during the freefall from both above and below the satellite, allowing for precise measurement of the relative rotational frequency. The measured rotational frequency was approximately **120RPM**, which aligns with the motor test results corresponding to a **0.52V** output voltage. The video from the test can be viewed here.

Another test was performed with the use of the Hall effect sensor and the motor output voltage divider. Thanks to these extra sensors, rotational frequency and generated voltage data was collected. Using a drone a controlled drop test was conducted from an altitude of **100 meters**.

The obtained data is plotted in **Figure 25**, the resulting graph shows an almost proportional correlation between motor voltage and rotational frequency, when taking into account the relatively high uncertainties involved in the experiment. Additionally, during the ascent phase, a

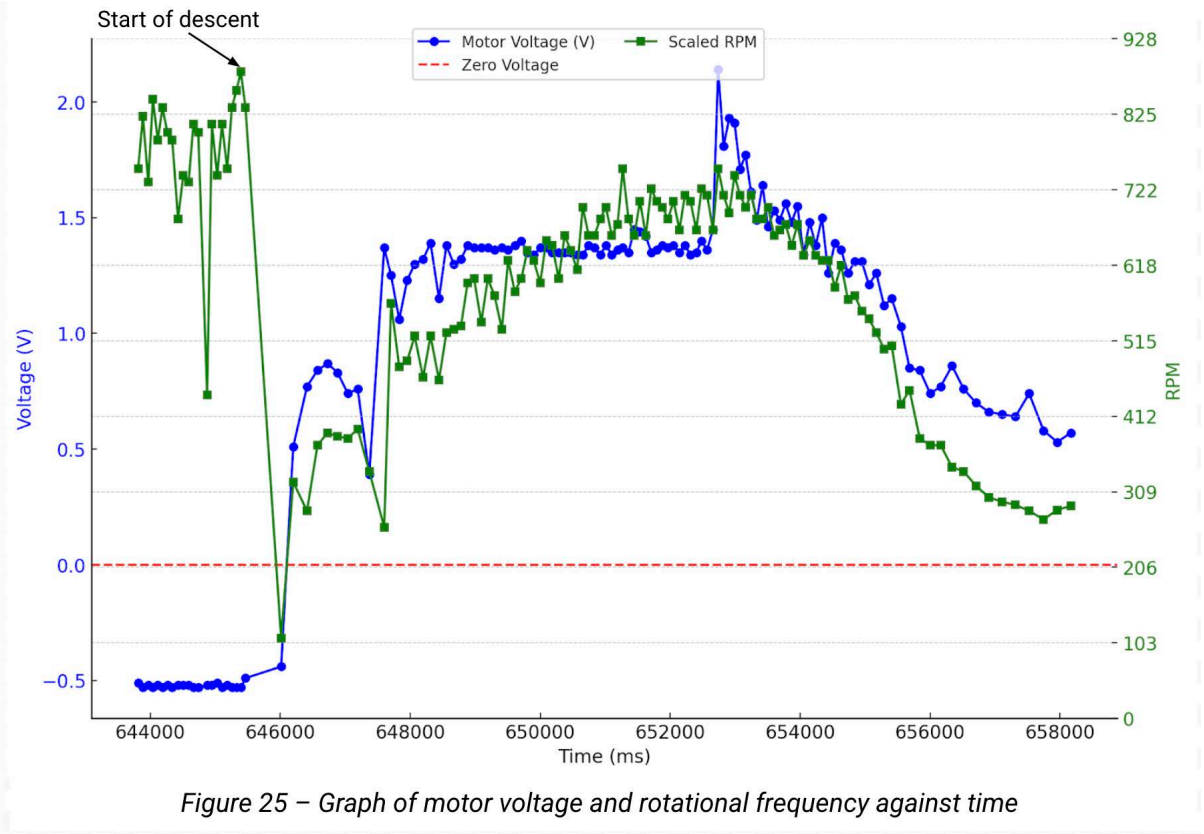

Figure 25 – Graph of motor voltage and rotational frequency against time

negative voltage is observed, which is indicative of the rotation of the CanSat's blades driven by the airflow generated beneath the drone. This proves that the blades cause rotary motion. Furthermore, higher altitude tests were performed, which proved that the lines would not tangle when falling. Test video is available here. Furthermore, they demonstrated that the actual rotational speed of the CanSat oscillates between 300 and 600RPM. Other tests have confirmed that energy **is indeed stored in the supercapacitor**. However, for the voltage and RPM measurements, the supercapacitor was disconnected, as it introduced a voltage drop that rendered the data unreliable. In earlier tests where the supercapacitor remained connected, the voltage typically ranged from **0.2V to 0.8V** due to the short duration of those tests (50–200 meters).

4.4 Mechanical Tests

As part of the test campaign, a series of mechanical tests was also conducted. The first of these was weighing all of the components one by one to establish the total mass of the CanSat. These results are presented in **Table 2**. The mass of **337g** is below the required CanSat mass, however, that is not a problem, since additional ballast will have to be added for even mass distribution within the CanSat. That mass will increase the potential energy thus the capacitor will charge to a higher voltage. A high altitude **drop test** was also conducted, by safely dropping the CanSat in a **controlled environment** from a **height of 100m** without a parachute. This test was thought out to check the durability of the CanSat body, even printed out of a less durable material than the final product, it managed to survive unscathed. Nonetheless, during the tests a different problem was revealed, while the body (**Figure 26**) is extremely durable, the blades suffered a different fate. While conducting the secondary mission tests one of the blades broke upon landing. To solve this issue **carbon rods** have been added to the blades of the CanSat (**Figure 26**). Implementing this measure proved sufficient, as there have been no problems with the durability of the blades even at higher-speed impacts with the ground, this proves that the mechanical aspect is **suitable for the mission**.

Part	Mass (g)
3D printed parts	173
Battery	44
Motor	31
PCB	22
Parachute	26
Bearings	12
Antenna	5
Supercapacitor	9
Carbon rods, screws	10
GPS	5
Total	337

Table 2 – Masses of parts

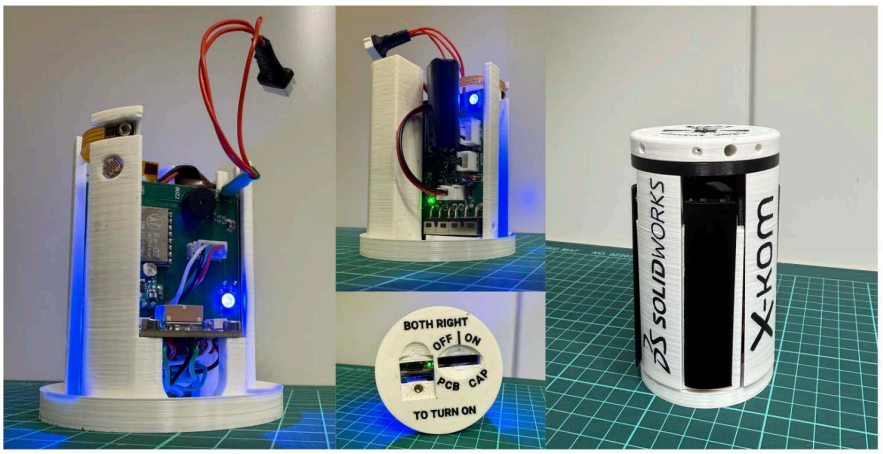

Figure 26 – Assembled CanSat

4.5 Communication System Tests

To ensure the proper functioning of the communication system a series of tests was conducted. The CanSat was attached to the drone provided by one of the sponsors of this project and the Received Signal Strength Indicator (RSSI) was measured at a plethora of distances, differing both in height and distance from the ground station. The RSSI

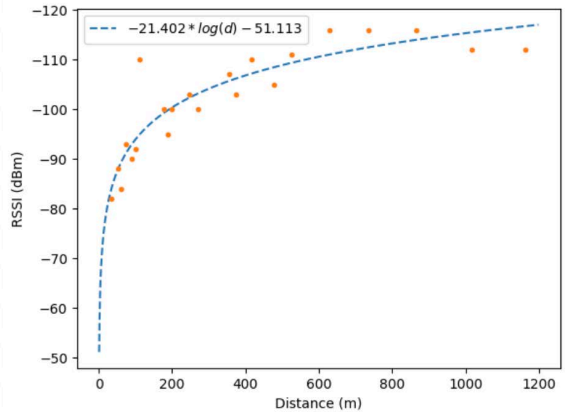

Figure 27 – RSSI against distance of the old antenna

is a common measure of signal strength, given as a negative integer, the closer it is to zero the better the radio signal strength. For the LoRa transmission to remain of a permissible quality the RSSI should not fall below -125. Below the results of the first test have been compiled and presented in **Figure 27**. One notable outlier may be noticed around (114, -110), this is due to the fact that in one test the antenna was not aimed correctly due to human error.

A logarithmic function has been fitted to the data collected using a gradient descent algorithm. The resulting function proves useful during maximum range calculations. Taking the equation:$RSSI(d) = -21.402\,log(d) - 51.113$, with d being the distance in meters, and assuming the minimum RSSI to be -125, the equation can be solved to acquire $d_{max} = 2833$ m. Since this does not leave enough allowance for CanSat drift as expected, tests with the Molex 204287-0050 antenna inside the CanSat have been carried out, with the results being presented in **Figure 28**. **1166 data points** were collected and a logarithmic function was fitted to the data using a gradient descent algorithm. Extrapolating the new function (visible in **Figure 28**) to a minimum RSSI of -125 yields a $d_{max} = 396$km, obviously this is not a realistic estimate of the CanSat range, since the antenna was aimed towards the CanSat and the logarithmic model does not truly reflect reality. Nevertheless, it does prove that the **Molex 204287-0050** is a better choice than the previous CanSat antenna and since a signal was received from 2500m without any problems the CanSat **more than satisfies the competition requirements**. Video from the test can be viewed here.

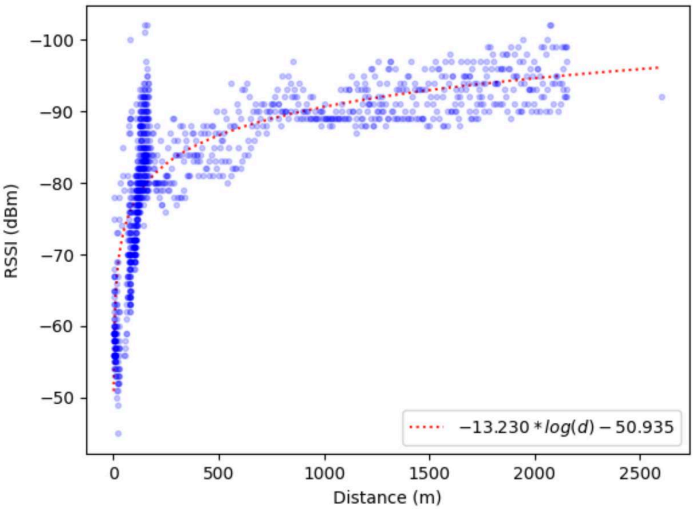

Figure 28 – RSSI against distance of the Molex 204287-0050 antenna

4.6 Recovery System Tests

CFD Simulations

Due to the irregular design of the parachute, **Computational Fluid Dynamics (CFD)** simulations in **Ansys Discovery** have been conducted to determine the optimal canopy size that would meet the competition's descent rate criteria for the CanSat. The objective was to adjust the descent velocity to the lower permissible boundary, aiming for slightly more than 5 m/s.

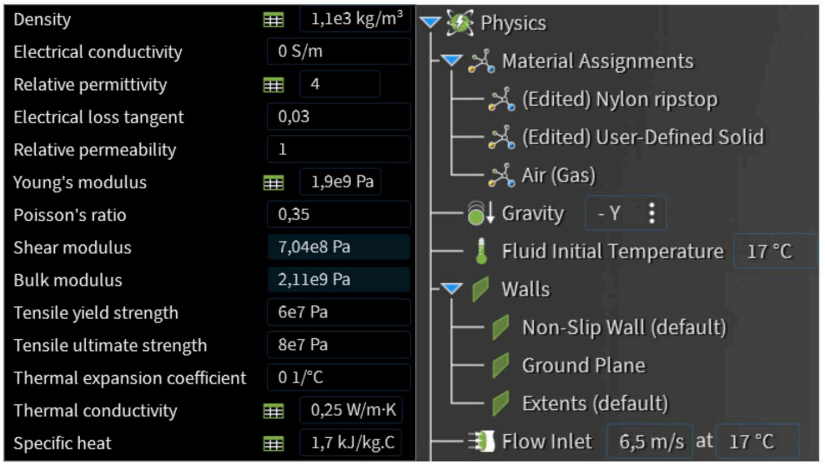

Figure 29 – Nylon Ripstop 40D material properties and the simulation boundary conditions and physical parameters

Mr. Jonathan Glanville **from Ansys**, Horsham, provided valuable advice to the team during an hour-long meeting and through email, helping achieve results that offer useful insights and reassurance. Therefore material properties, boundary conditions and physical parameters were set as visible in **Figure 29**. Mr. Glanville advised the team to use default meshing built in the Ansys Discovery program. This type of mesh gave the parachute properties similar to a rigid body. Even though it is not as accurate as an adjusted mesh, in the case of a fully deployed parachute canopy, it gives a picture that is close to reality. That is because the deployed canopy acts similarly to a rigid body (at least definitely more similarly than during the deployment stage). Moreover, Mr. Glanville gave the team a tip to create a space in the simulation with mass equal to the mass (~337g) of the satellite, so that it pulls the parachute down just like the satellite would. It is the User-Defined Solid in **Figure 29**.

After several iterations, the simulated air inlet velocity was set to **6.5m/s**. This value proved to be optimal for the parachute's configuration. The simulation results supported the previous assumptions, confirming that the approach to estimating the parachute's size was valid. While it is important to acknowledge that the CFD model represents an approximation of real-world behavior, it provided valuable insights and served **its primary purpose:** offering reassurance that the design was on the right track.

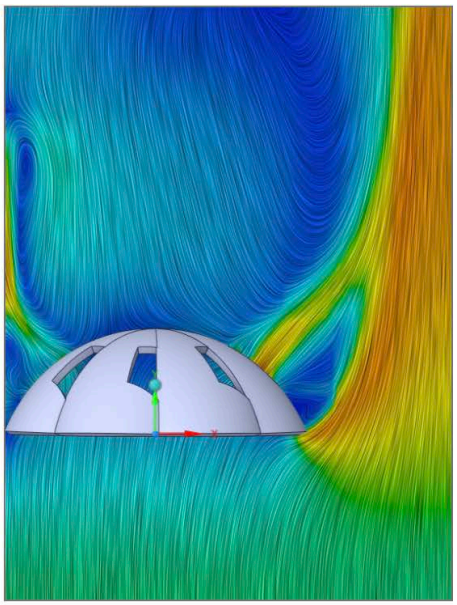

Figure 30 – Air flow velocities over the canopy

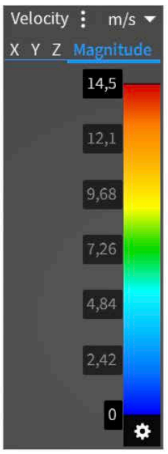

Figure 31 – Air flow velocities graph

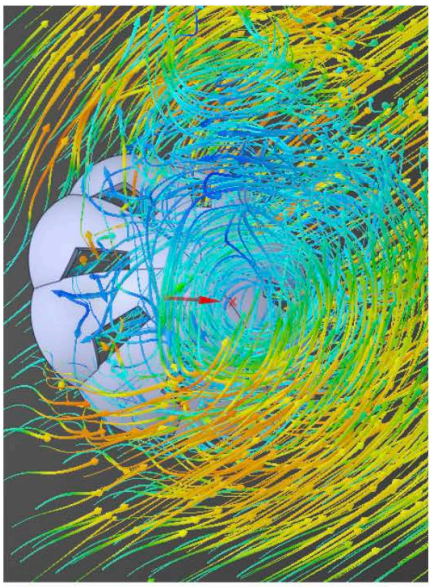

Figure 32 – Representation of the circular motion of the air flow over the canopy

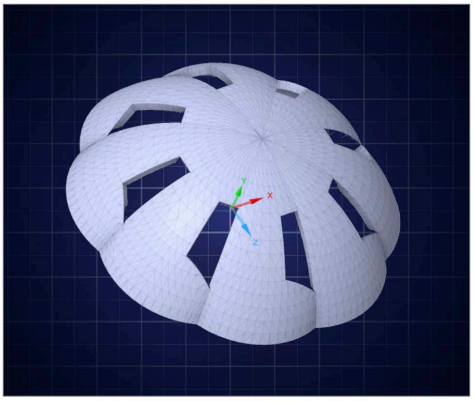

Figure 33 – Enhanced parachute mesh

A legend of velocities to the simulations has been attached in **Figure 31**. **Figure 30** illustrates the airflow over the parachute canopy, with specific air velocities in Figure 28. Notably, the air above the parachute experiences a significant reduction in velocity (except through the vents),

reinforcing the conclusion that the modeled parachute size is suitable for real-world testing.

In contrast, **Figure 32** highlights the circular motion of air above the canopy. This pattern further validates the design by confirming the rotational behavior of the parachute during descent. This rotational motion allows for the accumulation of energy, which could be utilized as part of the system's functionality.

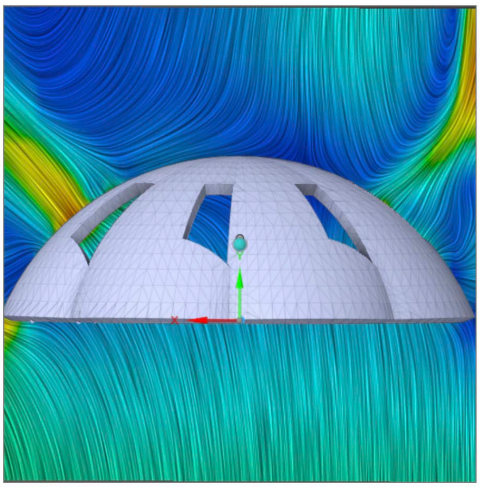

Figure 34 – Air flow over the parachute with enhanced mesh

After tests using a real parachute (described in detail in the next section), it was found that the rate of descent is slightly higher than the estimated one. After utilizing more complex meshing, the air inlet velocity was set to an optimal value of **7m/s**, showing that a non-rigid parachute descends faster than the more rigid version. The rigid parachute might maintain a more stable shape, producing higher drag, which results in a slower descent. The mesh in **Figure 33** consists of triangular elements, as created by Ansys Discovery's automatic meshing. The tool generated a uniform distribution of elements across the parachute canopy with a total of **8764 faces and 4324 vertices**, ensuring a balance between computational efficiency and resolution. The boundary conditions and parameters for the second simulation were the same as in **Figure 29**, except for the inlet velocity that was set to 7m/s (and of course the meshing was different).

Results of the simulation with (**Figure 34**) and without (**Figure 31**) complex meshing were really similar - except for the difference in the optimal settings for the air inlet velocity, there were no significant differences. In both cases the presence of a low-velocity wake region confirms that the parachute generates significant drag. The simulated inlet velocities of 6.5m/s and 7m/s suggest that the estimated descent rate is as desired previously **in the lower range of 5-12m/s.** However, as explored in the next section, the actual descent speed also depends on the specific balance of gravitational and aerodynamic forces that is apparent in the swinging of the parachute.

Rate of Descent Tests

The first real-world tests were conducted from an 8-meter tall launching platform, resulting in a flight time ranging from **1.20** seconds to **1.60** seconds. As anticipated, the recorded velocities (**Table 3**) were near the limit of the permitted values, as shown in the adjacent table. While the short flight time introduced some uncertainty in the measurements, all the results adhered to the contest's criteria. Overall, the outcomes were satisfactory.

Attempt	**1**	**2**	**3**	**4**	**5**
Result (m/s)	5.12	5.51	5.82	6.80	5.74

Table 3 – CanSat descent velocities

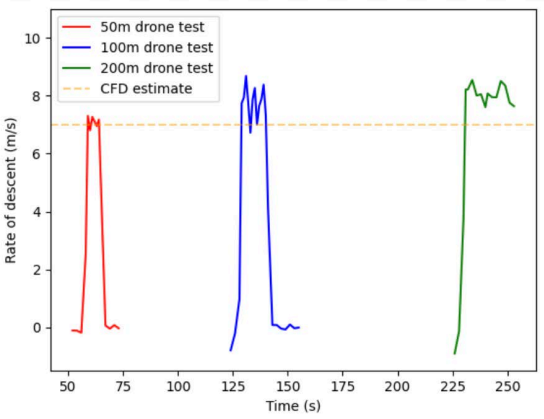

Figure 35 – Measured descent rate from several drop tests

Together with other tests conducted using the drone, the descent rate was measured at average **8m/s**, as seen in **Figure 35**. This value is slightly higher than what was estimated in the CFD simulations in the previous section probably because of the parachute's continuous swinging, which can be seen in the footage from the **drop test** here. While this value is higher than the predictions from simulations and earlier tests, several factors contributed to the significant difference:

- **Parachute swinging:** When the parachute, together with the satellite, swings, the parachute's effective drag area decreases for a moment, causing it to descend faster than without that effect.
- **Uneven mass distribution**: The uneven weight distribution in the CanSat further exacerbated instability in the final meters. This issue has already been addressed by remodelling the CanSat to fix any disparities.
- **Better reflection of reality:** The longer test gives a better image of what the rate of descent's value really is.

It is important to note that, considering these factors, the value of **7.5 m/s** is entirely acceptable for our project, as it falls within the specified **range of 5–12 m/s**. The current parachute size is unlikely to be modified in the future, as it represents an optimal balance between achieving a lower descent rate and avoiding excessive drift distance.

4.7 Energy Budget Tests

To check whether the estimates of the runtime of the CanSat are correct, a full energy budget test was conducted. The CanSat battery was charged to maximum capacity and the device was left in full operational capacity over the night. The CanSat was actively gathering data for the primary and secondary missions, indicating its state via 4 LEDs, saving the data on the SD-card, and transmitting it via LoRa to the ground station. The results have been compiled in **Figure 36** and the resulting battery voltage against time curve closely resembles a typical 18650 Li-Ion battery voltage discharge curve, with the upper and lower bounds corresponding to the specification of the chosen cell, confirming that the battery voltage measurements are correct. The CanSat functioned fully for over **406 minutes**, at a room temperature of 22°C. The results of

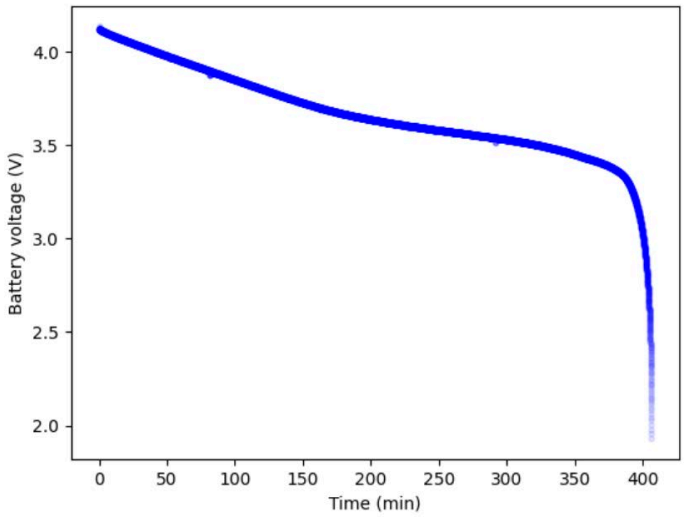

Figure 36 – Graph of battery voltage against time

this test almost perfectly match the estimate calculated in Section 3.4, this fact is quite surprising but there are two main reasons behind it. In the experimental test the buzzer was not switched on, hence decreasing power consumption, however the battery was also not fully charged, this fact may be deduced, since there is no sharp hook at the beginning of the graph in **Figure 36** and the starting output voltage was slightly lower than the value used in the calculations. The fact that these two figures only differ by half a minute is mostly serendipity, since two unrelated factors ended up balancing each other out, this is not to say that either approach was flawed, both the calculations and the experiment were designed to ensure the best results possible, taking into account as many factors as possible and avoiding unnecessary assumptions, rather the extent of the similarity between the values is befuddling, warranting the sacrifice of a few sentences to explain this phenomenon. Despite the fact that the temperature during the launch campaign will likely be lower, the total time until full discharge is expected to stay almost the same and will **fully satisfy the recommended value,** since it remains within the recommended temperature range of the 18650 Li-Ion battery.

4.8 High-Altitude Tests

In total, seven high-altitude drone tests were conducted: a **50m** drone test, two **100m** drone tests, three **200m** drone tests, and a **660m** airplane test, illustrated in **Figure 37**. These actions were undertaken to check the holistic functioning of the CanSat and ensure that all of the systems work together to fulfil the primary and secondary missions.

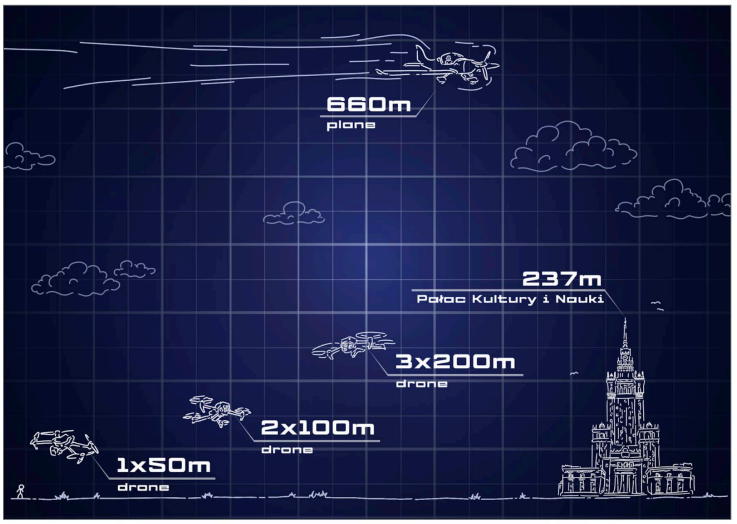

Figure 37 – comparison of tests' altitudes

Airplane Test

The general drop test was conducted on the 23rd of march 2025 through a cooperation with **WP Aero-Tech**, who provided an airplane to raise the CanSat to an otherwise unreachable altitude. The probe fell from 660m above the ground, which closely reflects conditions of the final flight in the rocket, therefore this trial can be assumed as the final check for all the systems.

Every sensor worked correctly during the whole fall, also the communication system transmitted data even on the ground, which enabled a successful recovery operation. The GPS system showed the location with a precision of 0.5m. The test of secondary mission devices was partially successful. Since the minimum flight speed of the airplane was over 100km/h. A flux of air at this speed caused a high overload on the parachute and blades. The canopy had to be folded on the side not top as during the launch campaign, which changed the way of opening. Simultaneous deployment of both systems caused the collision, this could have potentially disrupted the parachute stabilization phase. Moreover, the canopy starts spinning immediately after it is filled, therefore during the airplane test the parachute started its rotational movement when it was not

properly aligned with the axis of the main body. This effect resulted in an incorrect transfer of drag forces to the disc, hence the strings did not have the expected movement freedom and tangled. These problems will not occur during the rocket launch (even in similar drop velocities), because the parachute will be stored on top of the main body and open on the proper axis. Failure in this test enabled the development of procedures and changes to prevent similar scenarios from happening in order to ensure safe descent. Overall the test showed that the mission is **ready for the launch** and provided insight into what must be done to ensure a **safe and successful descent**.

Figure 38 – Photos of the drop test setup

Drone Tests

Better overview for the secondary mission was given by the drop tests from the drone, where in each one parachute and blades opened successfully, reaching the maximum rotational speed of up to 650RPM. Video from one of them (link). In smaller overloads the parachute stabilized correctly without causing strings to tangle. One of the sponsors - **X-kom** supplied a **drone for testing**, which the team equipped with a custom-designed dropping device **(Figure 38)**. All of

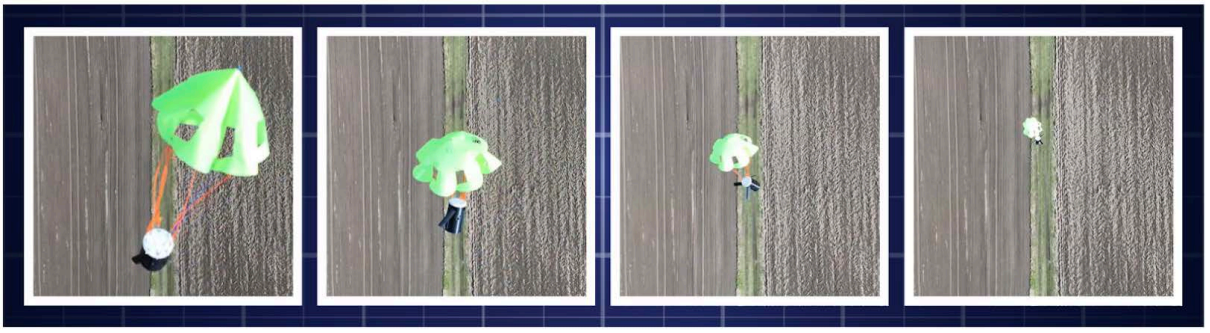

Figure 39 – The parachute and blades deploying successfully

our objectives from Section 2.3 were fulfilled:

- The parachute and blades opened successfully as seen in **Figure 39**.
- The parachute and CanSat body rotated in opposite directions as seen in **Figure 25**
- Electricity was generated (**Figure 25**) and stored in the supercapacitor (Section 4.3).

5 Project Planning

5.1 Time Schedule

Figure 40 – Project timeline

During the PDR stage of this project focus was mainly placed on developing ideas and writing the report. Nonetheless, a general plan has also been made, which illustrates the team's past, current and future tasks, by dividing the total competition time into six distinct stages. This schedule has been concisely presented in **Figure 40.** At the time of writing the CDR, the team has managed to exceed these initial predictions, being roughly a month ahead, having already finished some of the tests planned for February. As of the time of writing the FDR the team has managed to complete all of the planned tasks and thanks to the time gained at the CDR stage was able to commit more time to holistic system tests, which closely mimic the launch campaign ensuring that all components will work according to plan during the actual mission.

5.2 Task List

	Maciej Gała	Michał Mueller	Miron Kobylański	Michał Mrzyk	Jan Bodys
PDR	Electrical Design	Recovery System Design	Software Design	Ground Support Equipment	Social Media and Logo
	Mission Overview	Mission Objectives	Outreach Programme	Mission Objectives	Mechanical Design
	Mechanical Design (support)	Project Planning	Mission Objectives	Software Design	Graphic Design
CDR	PCB Board	Recovery System Tests	Outreach Programme	Mission tests	Social Media and Logo
	Electrical System Tests	Sponsors and Partnerships	Programming CanSat's Software	Ground Communication Tests	Refining the 3D Model
	Mission Tests	CFD simulation	Data analysis and debugging	Phisics analysis	Promotion in Schools
FDR	Final Mission Tests	Medial contacts	Ground station UI programming	Final Mission Tests	Social Media
	Assembling CanSat	Sponsorship communication	Finishing software	Further Communication Tests	3D model finishing touches
	Electrical System Tests	International promotion	Exploring WiFi capabilities of ESP32	Calculations needed for data analysis	School and event promotion

Table 4 – Task list

This list provides an overview of the tasks of each team member in the individual project stages. The team works closely together and their actions are closely interwoven so oftentimes more than one person is working on a specific task. This means everyone helps and advises the others. For example, the Recovery System is exceptionally intertwined with the Electrical System due to the secondary mission regarding taking in electrical energy. Because of that, the Electrical & Mechanical Team and Recovery Team have to closely cooperate with each other. Nevertheless, the main tasks each member will be focusing on have been outlined in **Table 4**. Thanks to thorough planning the team was able to avoid any delays or complications caused by setbacks in one field impacting another one. Proper organisation was even more important in this case since only two team members live near each other, and one even lives in a different time zone.

5.3 Achieving Sustainable Development Goals

The CanSat Competition is a unique event that **combines education, technology, and innovation,** offering participants the opportunity to apply their knowledge in engineering, natural sciences, and technology. It is a great opportunity to introduce **the Sustainable Development Goals** which young engineers should pursue.

Common points of SDGs and CanSat Competition program:

- **Goal 4: Quality Education** – competition promotes STEM education - during the work process we had gained a lot of practical skills that are essential nowadays
- **Goal 9: Industry, Innovation, and Infrastructure** - practicing engineering competences are the main pillar of space industries which has an increasing impact on everyday life
- **Goal 13: Climate Action** – the mission focus on recovering energy - renewable energy sources are the main target of the energy industry
- **Goal 17: Partnerships for the Goals** – one of the competition tasks is to find partnership and sponsors for the team. What follows is the ability to learn more about certain tools or programs that could help in designing the device.

By integrating sustainable development principles into satellite projects, young engineers can contribute to a better understanding and protection of the planet while inspiring others to take action for a sustainable future.

Link to SDGs map

5.4 Resource Estimation

All of the components were selected from the LCSC component library, thus all the exact prices of the components were known before ordering. The PCBs have been ordered and delivered, so exact price is known including delivery and duty cost. Mechanical part prices have also been estimated. The total cost per satellite is no more than **€250**, as shown in **Table 5**.

The minimum order quantity for PCB assembly was 5 units, requiring an upfront payment of €400. A beneficial outcome of this is the availability of 4 spare PCBs, one of which is used in the ground station. Additionally, ground support equipment, including a Yagi antenna, an additional ESP32 board, LoRa modules, and a laptop, have not been factored into the current cost calculations, they have however been displayed in **Table 6**. The total price of the ground station and a single satellite is €332,49. Sponsorships for a total of €700 have been secured providing a great reserve in case of any unexpected expenses. The project has additionally been selected as a

beneficiary of the "**Ochota Na Naukę"** grant, which provided additional funding of €380 for electronics for tests (supercapacitors, antennas, motors, sensors), as well as team hoodies and other promotion items.

Name	Euro price
Total PCB + components + assembly + delivery + duty cost	97,46
External GPS module - PA1010D Stemma QT	39,34
Supercapacitor 5F	10,55
Battery - Samsung INR18650	8,29
Parachute material	7,49
PC Polymaker filament 200g	4,68
Screws, inserts	4,55
TF card	4,12
CanSat internal antenna	7,89
Cables and connectors	2,23
Parachute cords	2,62
Dynamo motor	1,41
Carbon rods	1,41
Flex PCB	17,6
Temperature and pressure sensors	4,87
Total:	214,51

Table 5 – Costs of the CanSat parts

Name	Euro price
Antenna CDMA ATK-10	17,31
Total PCB cost	97,46
Antenna cables	3,21
Total:	117,98

Table 6 – Costs of ground station parts

6 Outreach Programme

This section is dedicated to describing the current progress and plans to improve the outreach programme, including social media, events in school, and collaboration with external media.

6.1 Brand Identity

The team's name was created to show the concept of the primary and secondary missions. It can be divided into two parts, with **"Re"** being connected to using one more time, which refers to the secondary mission **(reusing energy)**, while the **"Sat"** part gives a clear image of what will be constructed. A unique brand logo has also been made by a member of the team, which will be visible on social media and at events, where this project will be showcased. Furthermore, a special font and color palette have been chosen to increase brand recognisability, these motives are used on all social media posts and on the ground station live dashboard.

One of the team's first actions was to create an official email address (resat.team@gmail.com) for correspondence. Not only did this make keeping track of all of the social media profiles easy but also created a platform to communicate with potential sponsors and partners, as well as maintain general professionalism. Moreover, ReSat Team merchandise has been ordered in the form of hoodies in cooperation with a clothing brand.

6.2 Social Media

A core part of creating products is a strong social media programme. The team's internet presence is mostly created by an Instagram account (**Figure 42**), with a supporting Facebook page (**Figure 41**). Since the start of this competition the Instagram profile has reached 221 followers, with the most famous video receiving over 1000 views and the most liked post exceeding 75 likes. The outreach programme effectively reaches an ever increasing demographic. At this moment the account has reached **14 062 Instagram users**. The team's social media focus is placed not only on sharing progress but also on spreading knowledge and **educating followers** on the topics of astronomy, sustainability, energy generation, and general engineering. In an effort to reach an even larger audience, a new content form has been added - reels, which are short, roughly 45 second,

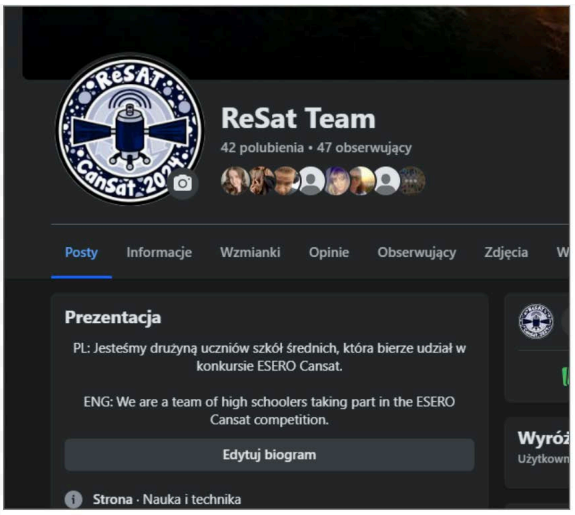

Figure 41 – The team's Facebook page

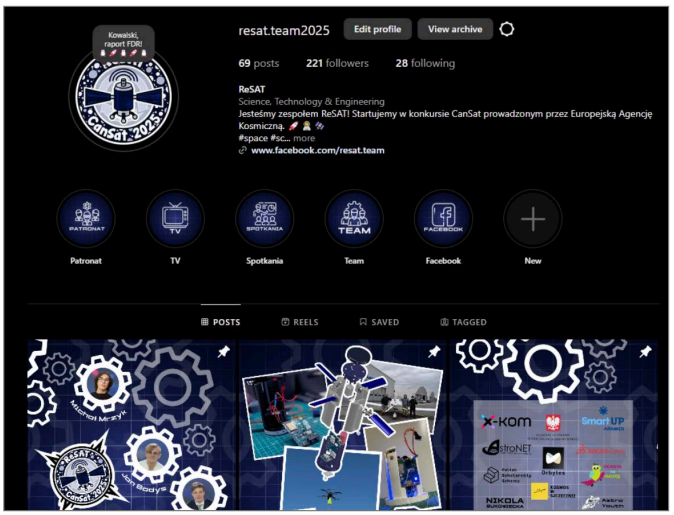

Figure 42 – The team's Instagram profile

long videos. Aside from an introductory reel, where the team members explained the ReSat principles and mission, two 8-reel-long series have been created and are currently being posted, one about different types of satellites and one about the life cycle of stars. Through these pieces of media **over 3000** people have been reached.

6.3 Promotion in Schools

Another crucial part of the outreach programme is in school promotion. As of the writing of this report the team members have visited three high schools to lead interactive workshops - SCI, IX LO in Szczecin, and XXXIII Dwujęzyczne LO im. Mikołaja Kopernika in Warsaw and one primary school - SP1 in Gryfino to present our mission to a total of over **550 students** and inspire them to take part in the CanSat competition in the future (link to photos). During these meetings the team members explained the premise of the CanSat competition, presented the basic engineering principles used in this project, highlighted the importance of proper planning and organisation, shared the ReSAT team values, and encouraged others to pursue their passions. Short notes on the respective members' schools' websites (click here and look for the article from 18.11.2024 -> link - for example. at Janek's school) have also been written. Plans for future development are regularly shared with our peers, who have become increasingly invested in this project even asking about the team's progress (click here). Additionally, the team members are spread across four different schools which gives the opportunity to reach a larger audience by simply informing classmates, for example a short talk was organised at Worth School visible in **Figure 43**. Finally, a workshop has been hosted at **Kopernikalia**, one of the biggest cultural-educational high-school festivals in Poland (click here). During the lecture, students could learn about astronomy, engineering, and the CanSat competition. This meeting was fully voluntary but all **100 available places** were booked only minutes after the sign-ups opened, this fact proves that there are many people interested in STEM, space, and technical projects, which proves that the outreach programme is a vital part of this endeavour.

Figure 43 – Support from the team's peers

Link to photos from all schools

6.4 External Media

Additional help will also be provided by the **sponsors** and **patrons** of this project, including organizations such as PSS (Polish Scholarship Scheme), X-Kom, Orbytes and one of the biggest Polish STEM scholarships - Adamed SmartUP. Their outreach is very broad and will surely bring a lot of attention to the project. Furthermore, the team's cooperation with external media also

included reaching out to online astronomy, engineering, and other related sites and blogs: Kosmos w Szczecinie, Nikola Bukowiecka, team Astro Youth and Astrofiyczka - Jowita Borowska-Naguszewska (link to stories). The team members actively participate in UKI (Uczniowskie Koło Informatyczne), the largest Student IT Club in Poland. This club has been used as a platform to further the reach of the outreach programme. AstroNET, the Polish Astronomy Portal, published an article about the project that has accumulated more than 600 views, shown in **Figure 44**. The team also appeared on TVP3 Szczecin, a local TV channel (13:15, Kronika), where they were able to reach people not normally interested in the STEM fields. During the segment the team members talked about their core principles, the ReSat mission, and the technical aspect of the project. Furthermore, after the appearance in the Western-Pomeranian local TV channel the segment was chosen to be shared to a nation wide broadcast (17:40). On the next day our performance was also released on national TV channel TVP info during the Teleexpress Extra edition (9:38). According to inside sources the joint viewership of these segments reaches anywhere between **400 thousand** and **750 thousand people.** A joint reel filmed with X-kom's media department is scheduled for the following two weeks. Our reportage was also uploaded on TVP3 Szczecin's TikTok account and gained almost 4 thousand views.

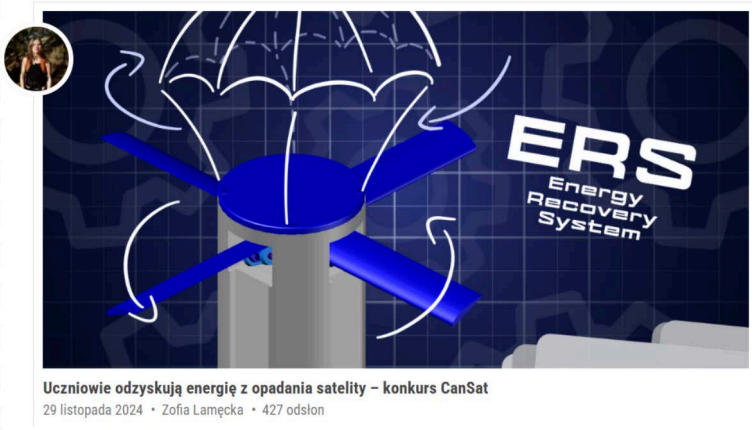

Figure 44 – Photo of AstroNET article

Links to TV program recordings

- TVP3 Szczecin - Kronika - https://szczecin.tvp.pl/85768977/2130-230225 13:15
- TVP3 Szczecin's TikTok account - https://www.tiktok.com/@tvp3szczecin/video/7485108385986153750
- TVP info - Dziennik Regionów - https://regiony.tvp.pl/85769086/dziennik-regionow-muzyczna-perla-regionow-tvp3 17:40
- TVP info - Teleexpress Extra - https://www.tvp.info/85388386/24032025-1715 9:38

6.5 Engagement with the Local Community

Throughout the project, we plan on heavily engaging with the team members' respective local communities; the hope is that this approach will allow the ReSat team to reach not only their peers but also younger and older members of society. For example, the workshop at SP1 in Gryfino, this presentation helped spur younger children's interest in astronomy and engineering as well as showed them an example project they could focus on. Even though this outreach programme is aimed at a broad audience, the most impactful actions will probably be the ones involving the local community, given their face-to-face nature. For instance, during the test campaign many people were interested in the CanSat. One of the most heartwarming moments during the drone

tests took place when a small crowd of curious villagers gathered to watch. Seizing the opportunity, members of the team gave an impromptu talk, sharing the purpose of the project and engaging in friendly conversation with the local community. This spontaneous exchange highlighted the true value of the outreach programme—not just in showcasing technology, but in building meaningful connections. For many who may not encounter astronomy or engineering in their everyday lives, this encounter offered a glimpse into the world of STEM, sparking interest and perhaps even inspiring future passions. Moments like these remind us how powerful knowledge-sharing can be, especially in places where such opportunities are rare yet so warmly received.

6.6 Sponsors and Patrons

The team has contacted and acquired several sponsors. As of the deadline of this Final Design Review the technical and financial sponsorship of X-Kom, Solidworks, the Adamed Foundation, and Orbytes has been secured. Moreover, a series of media patrons have also been acquired to help support the outreach programme: including: the Polish Scholarship Scheme, Astro Fizyczka, Nikola Bukowiecka, Astro Youth, AstroNET, and Space in Szczecin. Furthermore, the project has joined the “Ochota na Naukę” programme, which apart from providing necessary funding, has also given the ReSAT team the opportunity to consult with professionals and facilitated further development of the outreach programme. Additionally, the honorary patronage of the Voivod of Western-Pomerania, which helped the team solidify its mainstream media presence. Last but not least WP Aero-Tech provided a possibility to conduct the final drop test from an airplane.

7 CanSat’s Specification

Characteristic	Figure
Mass	337g
Diameter	65.50mm
Height (without parachute compartment)	114.50mm
Total cost	€214.51
Estimated time on battery (fully operational)	6.77h
Descent speed	8 m/s
Radio frequency	433MHz
Radio bandwidth	125kHz
Radio output signal strength	-27 dBm

Table 7 – Physical specification of the CanSat

Smart UP ADAMED

PATRONAT HONOROWY
WOJEWODA ZACHODNIOPOMORSKI

X-KOM

SOLIDWORKS

OCHOTA na NAUKĘ

Polish Scholarship Scheme

AstroNET Polski Portal Astronomiczny

Orbytes

KOSMOS W SZCZECINIE

NIKOLA BUKOWIECKA

Astro Youth

ASTRO FIZYCZKA

esa

esero